# Journal of Energy

ISSN 1849–0751 (On–line)
ISSN 0013–7448 (Print)
UDK 621.31

https://doi.org/10.37798/EN2022713

VOLUME 71 Number 3 | 2022

ENERGIJA 71

# Journal of Energy

**Scientific Professional Journal Of Energy, Electricity, Power Systems**
Online ISSN 1849–0751, Print ISSN 0013–7448, VOL 71
https://doi.org/10.37798/EN2022713

**Published by**
**HEP d.d.,** Ulica grada Vukovara 37, HR–10000 Zagreb
**HRO CIGRÉ,** Berislavićeva 6, HR–10000 Zagreb




# EDITORIAL

The first paper is "The Impact of Residential Optimally Designed Rooftop PV System on Libya Power Shortage Case". This study focuses on the potential of hybrid rooftop PV solar systems in Libya, where the average yearly hours of sunshine is 3200 hours and solar irradiance ranges from 6 to 7 kWh/m2/day. The aim is to mitigate the consequences of load shedding due to power shortages. A proposed 5.65 kWp PV solar system is suitable for Libyan households, aiming to gradually reduce reliance on oil for electricity generation. The benefits, simulation summary, and implementation approach are discussed. The significance of the proposed rooftop system is examined in Misrata, the third largest city in Libya. The simulation shows the peak load hitting 464 MW on September 9, 2019. PVsyst software is used for the simulation, considering that the grid compensates for energy shortages.

The second paper is "MAAP 4.07 Analysis of Long Term Containment Heat Removal after Reactor Vessel Failure (DEC-B) for Nuclear Power Plant Krško (NEK). This paper discusses the analysis of containment heat removal following reactor vessel failure caused by the initial Station Blackout (SBO) accident. Various mitigation measures are examined, including the use of alternative equipment such as the Alternative Residual Heat Removal (ARHR) pump and heat exchanger, as well as the Alternative Safety Injection (ASI) pump. The analysis follows the NEK Severe Accident Mitigation Guidelines (SAMG). Different options for heat removal from the containment are explored, depending on the availability of water sources and suitable heat exchangers. The results demonstrate that heat removal can be achieved through either injection to the Reactor Coolant System (RCS) or spraying the containment. The paper highlights the importance of early active containment heat removal to prevent fission product release.

The third paper is "Electric Vehicle Charging Infrastructure in Croatia – First-Hand Experiences and Recommendations for Future Development". This paper addresses the issues with electric vehicle (EV) charging infrastructure, including the lack of charging points and their inadequate power capacity. Additionally, the technology itself faces challenges due to insufficient testing, immaturity, and irregular handling. The study presents firsthand experiences of long-range EV trips originating from Zagreb, Croatia, in 2022. During the specific long-range trips, a Hyundai IONIQ 5 EV was used, covering distances that varied from 340 km to over 600 km. These trips predominantly took place on fast highways. The assessment focuses on the locations, power, and availability of charging points. Based on these experiences, the paper suggests possible directions for the further development of EV charging infrastructure in Croatia.

The fourth paper is "TARGET – Development of Submersible ROV System for BMN Inspection". This paper presents guidelines that encompass both visual and periodic non-visual nondestructive examinations to detect signs of service-induced cracking. Most pressurized water reactors (PWRs) utilize nickel-based Inconel Alloy 600 for in-core nuclear instrumentation penetrations in the reactor pressure vessel (RPV) lower heads. However, operating conditions in PWR plants can lead to primary water stress corrosion cracking (PWSCC) of these nickel-based alloys. In response to this issue, various inspection and evaluation guidelines have been developed, such as EPRI MRP-206, which provides guidelines for inspecting bottom mounted nozzles (BMNs) and detecting service-induced degradation. Mockup evaluations were conducted to further validate the UT technique and probe design. The results indicate that INETEC's system meets the requirements for flaw detection and characterization.

The last paper is „Bus Split Contingency Analysis Implementation in the NetVision DAM EMS". This paper describes the implementation of bus coupler outage scenarios in the NetVision DAM energy management system (EMS) contingency analysis. The existing topology processor was upgraded to identify bus coupler branches in the network model using a topological algorithm. Calculation subnodes were created based on the topology analysis results, and the calculation model was modified to include the bus couplers and subnodes as new calculation objects. These modifications are crucial for incorporating bus coupler outages in the contingency analysis. The mathematical analysis of the bus coupler outage scenario involves modifying input matrices and vectors to accommodate the increased number of calculation nodes. While refactorization of Jacobi matrices is necessary, it is a more efficient solution compared to creating a new calculation model from scratch. The implications of bus coupler outages on the load flow mathematical model are discussed, and the paper presents the implemented NetVision DAM solution for analyzing such outage scenarios.

**Igor Kuzle**
Editor–in–Chief

Journal of Energy

VOLUME 71 Number 3 | 2022

journal homepage: http://journalofenergy.com/

# The Impact of Residential Optimally Designed Rooftop PV System on Libya Power Shortage Case

Saleh Eshtaiwi, Mustafa Aburwais, Osama Elsanusi, Mustafa Elayeb, Mohamed Shetwan

***Summary* — The average yearly hours of sunshine in Libya reaches 3200 hours and solar irradiance rate approximately ranges from 6 to 7 kWh/m²/day. However, small solar parks projects are now undergoing and some are lately under cadastral and field survey. In meanwhile, $922.7M is the average annual government fund paid for electricity generation sector. It thus results in Tariff of 0.082 $/kWh. This paper studies the potential of hybrid rooftop PV solar systems to supply household appliances and then proposes a 5.65 $kW_p$ PV solar system appropriate for Libyan home's rooftop to mitigate the consequences of load shedding due to electric power shortage. Accordingly, oil uses in electricity generation will be gradually reduced as a result to rooftop PV systems widely spread. Finally, the overall benefits, simulation summery and implementation approach are provided.**

***Keywords* — hybrid, load shedding, PV solar system, rooftop, utility grid.**

## I. Introduction

The Libyan power plants rely only on conventional fuel such as heavy oil, light oil and natural gas. Those power plants are the main electricity supplier to the Libyan grid. The average efficiency of 6.4 GW generated power of aforementioned power plants is about 33% [1]. This much of energy requires about 3.5 million m3/year of heavy and light oil in addition to 6,531,492,999 m3/year of natural gas [1].

The fuel costs the government about $4.5 million per day [2]. As a result, the government is selling the electricity energy at a Tariff of 0.083 $/kWh. The government is funding and supporting the burned fuel by about 655-1,318 million dollars annually depends on oil and natural gas national prices [1], [2], [3].

Fig. 1 illustrates the amount of fuel that is consumed in the Libyan power plants in a period of 2013-2021 [4].

Throughout Libyan sectors, the residential sector has been found consuming the most see Fig. 2.

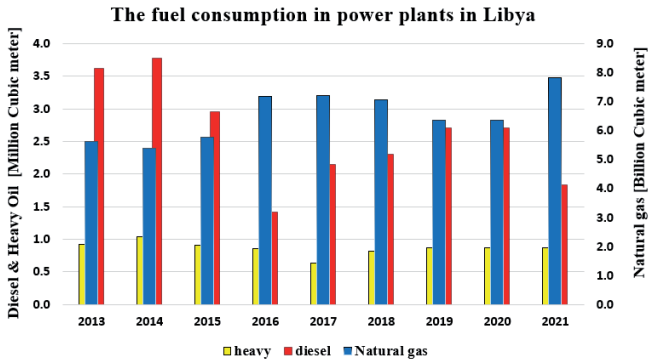


Fig. 1. The fuel consumption in power plants in Libya

At the residential sector, Population growth and high standard living achieved in the last decade could be the main reason of high percentage of electric energy consumption. The higher consumption of electric power increases the power demand to around 8 GW with an estimated shortage of 1.6 GW [4].

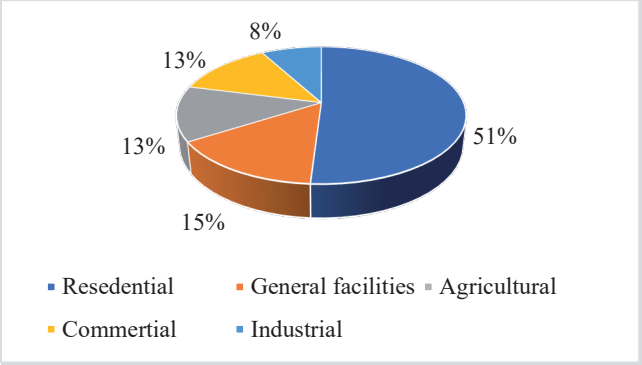


Fig. 2. The electricity energy consumptions of Libyan sectors

Formerly, the country vision was only limited to found new conventional power plants, which necessitates a great investment as well as long time is required, while no serious effort toward the available sustainable energy resources. However, Libya has elevated solar irradiance reaches 2300 kWh/m²/year and sunshine duration is near 3200 hr/year [5], compared to other world countries, who has smaller amount and have made a great trade in the field. For instance, China vision by 2030 is to exceed 26% of renewable energy sources [6]. Meanwhile the United States of America goal is to achieve 22% of their generated power from renewable

(Corresponding author: Saleh Eshtaiwi).

Saleh Eshtaiwi is with the General Electricity Company of Libya (GECOL), Tripoli, Libya (saleheshtaiwi@ ku.edu).

Mustafa Aburwais, Osama Elsanusi and Mustafa Elayeb are with the Misurata University, Misrata, Libya (mustafa.elayeb@eng.misuratau.edu.ly).

Mohamed Shetwan is with the College of Industrial Technology, Misrata, Libya.

"This work was carried out by the support of Misrata Municipal Council."

energy resources [7], [8]. In Libya, the current instability in a political environment have posed a great challenge to the General Electricity Company of Libya (GECOL) who became unable to overcome the escalated growth in power demand. Therefore, GECOL is daily scheduled a load shedding during summer season as a precaution to prevent a complete blackout. Nowadays, the GECOL has lately started an investment in PV solar parks. It newly has signed agreements and contracts with some international companies, such as TotalEnergies and EG. TotalEnergies will start a project of 500 $MW_p$ solar park in Sadada region (around 70km east of Misrata city) and a capacity of 200 $MW_p$ with the EG company in city of Ghadames (300km south of Tripoli) [6].

In this study, rooftop PV system is carried out to get it installed in 100,000 houses all over Libya. The system is going to be simulated to supply the residential sector and come over the electricity shortages. A case study in the city of Misrata is simulated and analyzed. Misrata is the third largest city after the capital city of Tripoli and the second city of Benghazi. Misrata is located in northwestern of Libya, situated 157 km to the east of Tripoli and 825km west of Benghazi on Mediterranean coast. The latitude and longitude of the city are 32.4° and 15.1° respectively, and the elevation is 10m.

## II. Rooftop Solar Systems

The residential and general facilities loads exceeds 66% as shown in Fig. 2, which is the largest consumers compared to the other sectors as revealed in [7], [8]. The potential of installing PV systems on house's rooftop was also discussed. It is a promising approach to avoid an expected grid black out because of power shortfall in Libya. The solution suggests that the national grid is used along with solar panels to feed the household appliances through a hybrid inverter (no power injected into grid) [4]. This is an effective scenario since the implementation is going to be easy to install, and fast to get it run. It simply guarantees the continuity operating of all necessary household loads. Certainly, it will gradually strengthen the concept of grid independence, actively change Libyans' consumption behavior and encouraging saving the national resource. It will also localize a new environment-friendly technology in addition to limits dangerous spread of backup generators. Furthermore, in upcoming future, rooftop systems can hereafter sell the electric power to the public grid, whenever an appropriate legislation (regulations) and infrastructure become available.

### *A. Components of Photovoltaic Solar System*

In Libya, the available PV panels today have a commercial dimension of approximately 2 $m^2$ to produce about 535$W_p$ with a lifespan of at least 25 years. Trina Solar has lately revealed a capacity of 600$W_p$ [9]. The panels produce a DC, and then an inverter is required to run the AC loads. While load shedding, the panels should be connected to a battery bank to meet the energy demand at night [10], [11], [12]. The process of batteries charging and discharging is usually carried out by means of a controller. In modern models, the intelligent controller is integrated into a hybrid inverter which can be programmed to set the priority of feeding the load whether from PV panels, grid, or batteries as shown in Fig. 3.

### *B. The Advantages of Rooftop Systems:*

- The PV system is only designed to feed the house, so no government regulations are needed.
- No land allocation is required from the state of Libya since the installation is on house's rooftop.
- The project (proposal) costs the state of Libya nothing neither operationally nor security obligations since it is under owner's care and responsibility.
- The project can noticeably make a change on the owner's life routine since the installation and setup takes a few hours, and power supplying will start immediately.
- For installation, no highly proficient technicians from abroad are needed, and therefore systems can be installed by local technicians after receiving a simple training.
- While backup generators are only start running once load shedding scheduled, rooftop systems are designed to permanently supply power to household appliances and as number of installed systems increase, power shortage decreases.
- As much as installed systems rises, the outcome is founding an equivalent conventional power plant at no government fund.
- In a case of citizens' financial hardship, only part of the essential loads can be basically fed, and then rooftop system's size can be expanded later as individual's economic conditions might improve, or because of technology development, prices may essentially decrease.
- The spread of rooftop systems will absolutely trigger the labor market as well as improve local economic conditions since it will offer more job opportunities in terms of installation and maintenance.
- PV system is confidently not source of noise, air pollution, or natural resources depletion, it basically requires a little maintenance within 5-10 years.

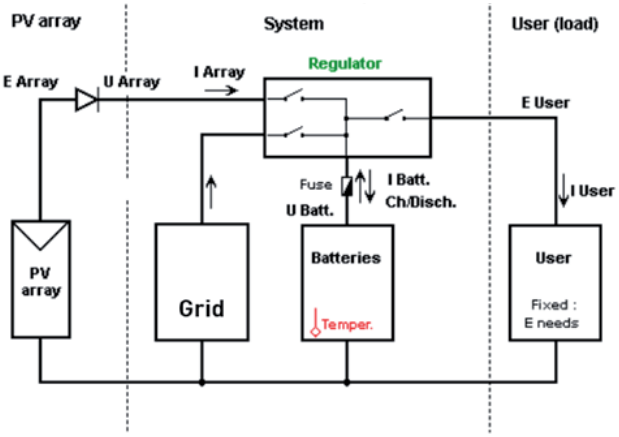


Fig. 3. Proposed PV solar system

The battery lifespan varies between 3-5 years depend on the DOD% while the lifespan of the inverters has exceeded 15 years [4],[13],[14]. The system's lifespan is more than enough for the GECOL to come up with a solution. One of effective solutions is approving new legislation that is feeding the grid through bidirectional meters [15]. In reality, new private companies have already launched to import and install PV systems besides offering ancillary services such as maintenance, developing technology, and equipment (modules and batteries) recycling [4].


Saleh Eshtaiwi, Mustafa Aburwais, Osama Elsanusi, Mustafa Elayeb, Mohamed Shetwan, The Impact of Residential Optimally Designed Rooftop PV System on Libya Power Shortage Case, Journal of Energy, vol. 71 Number 3 (2022), 3–9
https://doi.org/10.37798/2022713377

## III. Typical House Daily Consumption in Libya

Actual measurements were obtained from GECOL based on randomly selected Libyan houses and were recorded by using the *VIP System3- energy analyzer*. It measures the actual consumption of the traditional Libyan houses. Fig. 4 displays real household consumption within 24 hrs.

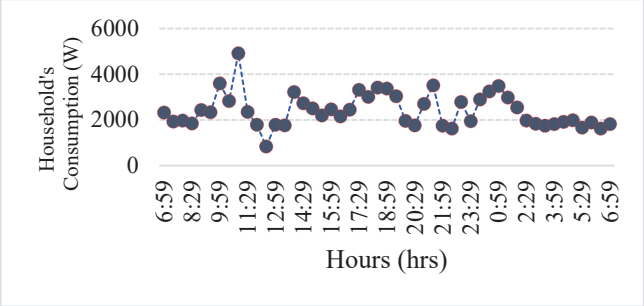


Fig. 4. Actual household consumption during 24 hours (daylight and night time)

From Fig. 4,5 and (TABLE I), it can be clearly noticed that the total consumed energy is completely unacceptable to get it supplied by using PV systems due to unconvincing cost, limited rooftop area and therefore our proposal is only restricted to the necessary household appliances as described in (TABLE III).

The real consumption can be summarized for the selected model (house), as shown in (TABLE I).

Table I

Actual Consumption of House on Libya

| Total rated power of household loads (kW) | Maximum actual household consumption Power (kW) | Daytime household consumption (kWh) | Night household consumption (kWh) | Total (kWh) |
|---|---|---|---|---|
| 11.598 | 4.918 | 25.6 | 30 | 55.6 |

## IV. Sizing Rooftop System

The appropriate size of rooftop solar system should be chosen to supply the household loads which are available on the most of the Libyan traditional houses. The final selected size should be feasible technically and economically and as a result, three different scenarios were studied:

### A. Scenario (I):

The PV solar system is sized to supply all household appliances and fulfill the customer needs. The home study model was measured by the *VIP system3*, in (TABLE I).

On (TABLE II) it can be obviously realized that the suggested PV system will have a large capacity, and high rate of battery discharge. It results in a high cost and probably becomes impossible to install due to limited roof area. Therefore, the model has been excluded at this stage.

Table II

Specification PV System of 1st Scenario

| System Component | Total Capacity | Qty | Note |
|---|---|---|---|
| PV panels | 535**W** | 20 | Well-matched system's component should be selected and appropriate to Libyan environment (temperature, dust, wind speed …etc) |
| Deep cycle batteries (DOD 60%) | **200**Ah, 12V | **12** | |
| Inverter | 10 kW | 1 | |

### B. Scenario (II):

In this scenario a PV system will supply household basic loads and neither an air conditioner nor heating appliances were included. Their power consumption is too high; therefore, an inverter air conditioner and domestic water heating are really recommended [4]. The details of each PV system components are as shown in (TABLE III) [4].

Table III

Specification PV System Of 2nd Scenario

| System Component | Total Capacity | Qty | Note |
|---|---|---|---|
| PV panels | 535Wp | 6 | Well-matched system's component should be selected and appropriate to Libyan environment (temperature, dust, wind speed …etc) |
| Deep cycle batteries (DOD 75%) | 200Ah, 12V | 4 | |
| Inverter | 3 kW | 1 | |

### C. Scenario (III)

In scenario *(III)*, studying the effect of adding only one highly efficient inverter air conditioner with a capacity of 12kBtu/h (no more than 700W) is analyzed. The consumption will slightly increase compared to the 2nd scenario, and thus the components of the system also increase. They are verified in (TABLE VI), which requires an increase in the PV modules and battery's storage capacity. This scenario is providing all household utilities with enough energy. However; legislation by government is needed to prevent using traditional air-conditioners.

Table IV

Specification PV System of 3rd Scenario.

| System Component | Total Capacity | Qty | Note |
|---|---|---|---|
| PV panels | 565Wp | 10 | Well-matched system's component should be selected and appropriate to Libyan environment (temperature, dust, wind speed …etc) |
| Deep cycle batteries (DOD 75%) | 200Ah, 12V | 8 | |
| Inverter | 5kW | 2 | |

### D. The Proposed PV Rooftop System

Based on the above-mentioned three scenarios, the scenario (III) was preferred and selected. The PV hybrid system provides the required energy to Libyan household's appliances. The PV system size will be limited to supply loads shown in (TABLE V). It reduces the inconvenience in case of scheduled power cut off with the possibility of developing, the rooftop system later on to be on-grid.


Saleh Eshtaiwi, Mustafa Aburwais, Osama Elsanusi, Mustafa Elayeb, Mohamed Shetwan, The Impact of Residential Optimally Designed Rooftop PV System on Libya Power Shortage Case, Journal of Energy, vol. 71 Number 3 (2022), 3–9
https://doi.org/10.37798/2022713377

TABLE V

THE EXPECTED BASIC LOAD FOR 3RD SCENARIO

| Appliances | *Rated kW* | *No* | *∑kW (max)* | Hours/day Used | | *Energy/day kWh* | |
|---|---|---|---|---|---|---|---|
| | | | | *Daytime* | *Night* | *Daytime* | *Night* |
| Fridge | 0.25 | 1 | 0.25 | 6 | 2 | 1.5 | 0.5 |
| Freeze | 0.25 | 1 | 0.25 | 6 | 2 | 1.5 | 0.5 |
| Lamps | 0.025 | 30 | 0.75 | 1 | 3 | 0.75 | 2.25 |
| Washing water pump iron | 1.5 | 1 | Programming (One per day) 1.5 | 2 | - | 3 | - |
| TV/PC/ Electric intake | 0.1 | 6 | 0.6 | 3 | 3 | 1.8 | 1.8 |
| Air conditioner | 0.7 | 1 | 0.25 | 8 | - | 5.6 | - |
| Total | | | 3.35 | | | **14.5** | **5.05** |

Proposal Hypotheses

- The government needs to fund 100% of system total cost, while the ownership is going to be transferred to the citizen within 5 years (which is enough for refund)
- The citizen is encouraged to afford the installation and maintenance fees.
- The citizen should change the traditional air conditioner to highly efficient inverter air conditioner.
- The citizen will be able to feed the grid once the regulations are approved to allow GECOL to buy the supplied energy.

In order to extend system life, it is recommended to literally take into account the following points:

1. Directing the consumers towards energy-saving and highly efficient appliances to apply the concept of energy efficiency. It is highly worth it if current household loads are replaced regularly by highly-efficient appliances.
2. Mainly, the daytime is the most appropriate time for consumption thus, the consumers should be aware to have most of their activity done at daytime.
3. Avoid excessive consumption, especially during the night time, due to side-effect on the battery's lifespan as long as the batteries represent the highest weight in the system's cost.
4. Only operate the recommended appliances and avoid heavily power consuming ones to extend batteries' life.

## V. CASE STUDY

In this paper, the significance of the proposed rooftop system will be studied in the city of Misrata, which is the third largest Libyan city. It is almost 210 km east of Tripoli and on the southern coast of the Mediterranean Sea. The curve shown in Fig. 5 illustrates the loads in Misrata which is daily fed from the GECOL's utility grid during the year of 2019, where it shows the maximum peak hitting 464 MW on September 9 of 2019.

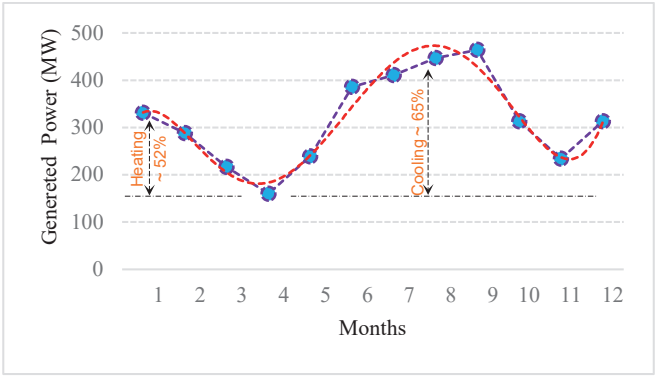


Fig. 5. The loads in the City of Misrata 2019

The simulation was carried out by PVsyst software for the proposed PV system on the Libyan case. In our scenario, it should be noted that the grid is going to compensate the energy needed of house utilities whenever a shortage happens of the system. The solar fraction in (TABLE 6) confirms that the obtained data can be used for economic calculations as well.

During the simulation, PVsyst software updates its meteorological data for the whole year based on the location of the proposed rooftop solar system. The data should include the horizontal global irradiance (GlobHor), horizontal diffuse irradiance (DiffHor), clearness index, ambient temperature, and wind speed. For city of Misrata, the latitude is (32.375°, 15.0915° longitude), GlobHor is 1755.3 kWh/m² /year, DiffHor is 831.3 kWh/m²/year, clearness index is 0.556, ambient temperature is 21° C, and wind speed is 4.3m/s.

From the PVsyst software simulation of the third *Scenario*, the total number of required batteries are 4 in order to meet the energy demand. The proposed battery is a 200 Ah with a nominal voltage of 12V for each. The battery has coulombic efficiency of 97%. Additionally, the batteries are expected to have the capability to supply the expected loads for one day. There are 10 PV modules to satisfy PV array configuration and used to electrify the loads besides charging the required batteries. The PV array is expected to generate nominal power around 5.65 $kW_p$. The proposal's design considers that the PV module output changes based on solar irradiance, ambient temperature and load demand.

In PVsyst software, the inverter and MPPT charge controllers are part of the regulator configurations. The nominal voltage is 48V. The selection is made based on system voltage on the battery storage. The controllers can regulate up to 5.65 kW of the maximum output power received from the batteries. From the simulation analysis results, the average unused energy is 1.1 $kWh/kW_p$/day, collection loss is 0.71 $kWh/kW_p$/day, system losses and battery charging are 0.56 $kWh/kW_p$/day, and energy supplied to the user is 2.85 $kWh/kW_p$/day.

In Fig. 5, the normalized energy production, which is distributed all over the year, is verified. The highest generated energy production is up to 6.2 $kWh/kW_p$/day and would happen from July and August. The main reason for high consumption is the traditional air conditioner as well as water heater. On the contrary, the lowest production will happen in winter from November to January with amount above 2 $kWh/kW_p$/day. As shown in Fig. 6, the most losses of PV modules occur in July, and August. Further, the highest unused energy plainly seen on May, June and July, respectively


Saleh Eshtaiwi, Mustafa Aburwais, Osama Elsanusi, Mustafa Elayeb, Mohamed Shetwan, The Impact of Residential Optimally Designed Rooftop PV System on Libya Power Shortage Case, Journal of Energy, vol. 71 Number 3 (2022), 3–9
https://doi.org/10.37798/2022713377

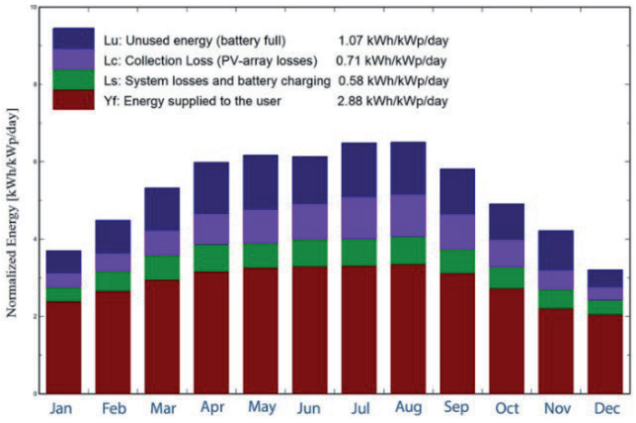


.Fig. 6. Monthly energy production with losses.

Fig. 7 reports the Performance Ratio (PR) within a year. PR is the system efficiency during the year and gives information about the impact of overall system losses on the rated output. The losses include PV module, tilt angle, dust, shade, as well as module temperature losses.

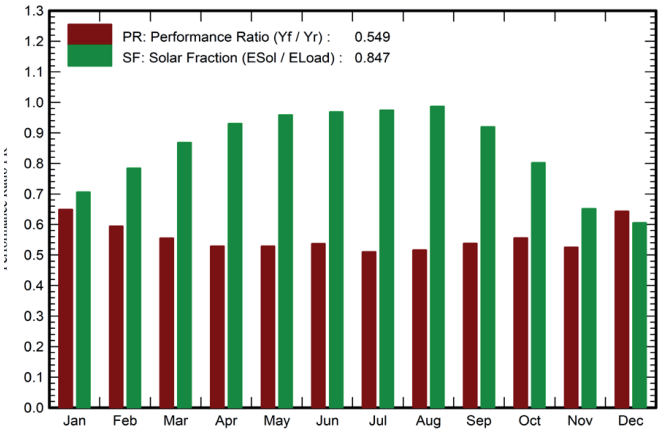


Fig. 7. Performance ratio and solar fraction using PVsyst.

Results using monocrystalline silicon PV modules indicate that throughout a year, the system exhibits a fluctuation, while solar fraction has experienced an increasing trend in the first four months of the year. Then, it has remained constant for two months and a rise in the next two months. Finally, a decreasing trend has occurred in the last four months of the year.

## VI. Estimated Costs of the Proposed System

Based on the selected rooftop system the obtained energy from a 5.65 $kW_p$ PV system is going to be very sufficient with slight back-up from grid to compensate any shortages to ensure smooth system operation. Therefore, the significant home appliances can be supplied via PV system described in (TABLE III), and its estimated cost is roughly $4,300.

## VII. Financial Support for solar systems

The paper recommends that $430 million should be annually assigned to the total cost of 5.65 $kW_p$ rooftop solar systems. It will effectively lead to installing a PV system in almost every Libyans household within 7 years. It may be useful to establish investment fund to support the proposal throughout additional public fund from other institutions such as, telecommunications companies, banking sector, and heavy power consumers from both public and private sectors. It is considered as financial compensation for their high consumption of subsidized electricity.

The installation of proposed project will visibly save the government support which is frequently paid to fund all kind of fuel used in traditional power plants, and it can be partially forwarded to yearly support such solar systems proposal.

## VIII. The Proposal's Outline

The proposal initially aims to install 100,000 systems with a capacity of 5.65 $kW_p$ within a year at a rate of 400 systems/day.

It further requires a training of 1056 people for installation progress. The cost of such systems is estimated to approximately $430 million. The Libyan government bears 100% of total cost. (TABLE VII) summaries the simulation and the study of the proposal.

Table VI

Energy Use

| | EArray kWh | E_Load kWh | E_User kWh | E_BkUp kWh | SolFrac ratio | T_LOL Hour | Pr_LOL % |
|---|---|---|---|---|---|---|---|
| January | 484.5 | 595.9 | 593.4 | 168.3 | 0.713 | 0 | 0.00 |
| February | 509.5 | 538.3 | 533.8 | 98.0 | 0.810 | 0 | 0.00 |
| March | 628.6 | 595.9 | 591.0 | 59.3 | 0.892 | 0 | 0.00 |
| April | 659.9 | 576.7 | 569.8 | 32.5 | 0.932 | 0 | 0.00 |
| May | 690.2 | 595.9 | 589.1 | 7.7 | 0.976 | 0 | 0.00 |
| June | 668.0 | 576.7 | 569.1 | 17.3 | 0.957 | 0 | 0.00 |
| July | 687.8 | 595.9 | 588.6 | 16.3 | 0.960 | 0 | 0.00 |
| August | 712.0 | 595.9 | 587.6 | 0.0 | 0.986 | 0 | 0.00 |
| September | 642.9 | 576.7 | 570.2 | 31.5 | 0.934 | 0 | 0.00 |
| October | 549.4 | 595.9 | 591.4 | 128.4 | 0.777 | 0 | 0.00 |
| November | 455.0 | 576.7 | 573.3 | 197.5 | 0.652 | 0 | 0.00 |
| December | 381.6 | 595.9 | 594.9 | 277.3 | 0.533 | 0 | 0.00 |
| Year | 7069.4 | 7016.8 | 6952.2 | 1034.0 | 0.843 | 0 | 0.00 |

## IX. Expected Proposal Benefits

### A. Libyans Citizen's benefit

Libyans who obtained such a PV system with an installed capacity of 5.56$kW_p$, are going to offer an annual electrical energy of 48.7MWh, which is sufficient to run all of the important appliances in typical Libyan houses, including highly efficient invertor air conditioner. The system is hybrid whenever there is no enough power at the PV system the grid will feed compensate the loss. Fig. 8 shows the annual back-up energy that is required from the grid compared to the solar power generation. It is clear that the first four months and last three months of the year there is back-up needed while slight to no back-up is needed for April, May, June, July and August. The annual back-up energy is estimated to be 1073 kWh

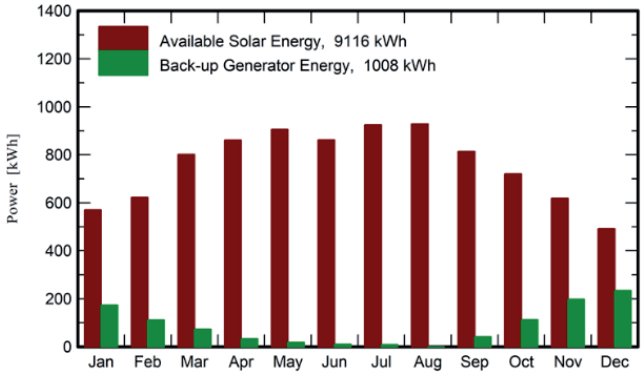


Fig. 8. The annual back-up energy required for one system compared to the solar power generated


Saleh Eshtaiwi, Mustafa Aburwais, Osama Elsanusi, Mustafa Elayeb, Mohamed Shetwan, The Impact of Residential Optimally Designed Rooftop PV System on Libya Power Shortage Case, Journal of Energy, vol. 71 Number 3 (2022), 3–9
https://doi.org/10.37798/2022713377

The available annual solar energy of the system is estimated to be 9116 kWh while the annual energy need of the user is estimated to be 7,017 kWh as shown in Fig. 9. It is clear that there is no back-up needed. However; the collection loss, system losses and battery charging made the back-up compulsory (see Fig.6 and Fig. 10).

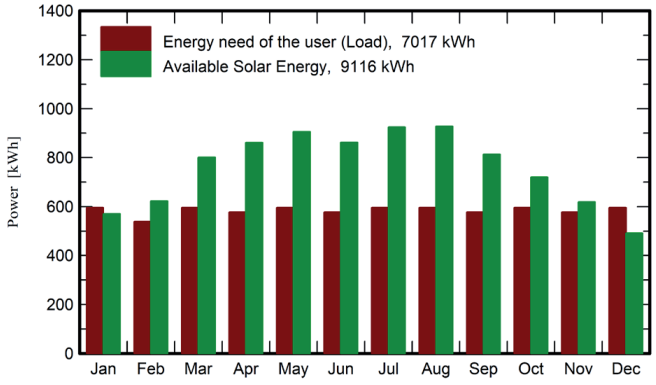


Fig. 9. The available solar energy to energy used of the user

TABLE VII

SIMULATION SUMMARY

| | |
|---|---|
| No. of installed PV solar Systems per year | 100,000 |
| Total installed power per year ($MW_p$) | 565 |
| The delivered energy per year (GWh) | 600.9 |
| The total supplied energy cost in case of traditionally generated ($ annually) | 132,198,000 |
| The average decreasing in $CO_2$ emissions per year, in case of conventional power plants generation (tons) | 390,585 |
| The average decreasing in $CO_2$ emissions per year, when using common backup generators (tons) | 480,720 |
| Averaged daily installed PV systems (250 workdays a year) | 400 |
| No. of installation teams (3 technicians each team) | 264 (792) |
| No. electric technicians' team (2 technicians each team) | 132 (264) |
| (Job offers, No. of expected trainees) | 1056 |
| The total PV systems estimated cost million Dollar | 430 |
| Total estimated cost of installation, $ (Based on 300 $ each) | 30,000,000 |

## B. Benefits into GECOL's Grid

Installing 100,000 rooftop solar systems means adding 565 MW to the installed capacity generated power. According to GECOL, the household sector is the largest energy consuming side, as it reaches 51% of the total sold energy [7],[8]. Therefore, targeting such sector is achievable by rationalizing and installing rooftop solar systems. It will have a realistic impact in terms of covering some of power demand besides enhancing grid stability.

## C. Environmental Benefits

According to [1], the average efficiency of the currently operated power plants in the Libyan public grid till 2022 have not exceed 33.3%. This means that 66.7% of the consumed fuel in power plants are wasted, and the lost rate reaches about 2275 million of the fuel subsidies assigned to the GECOL in the same year. It results an emission of about 23 million tons of $CO_2$.

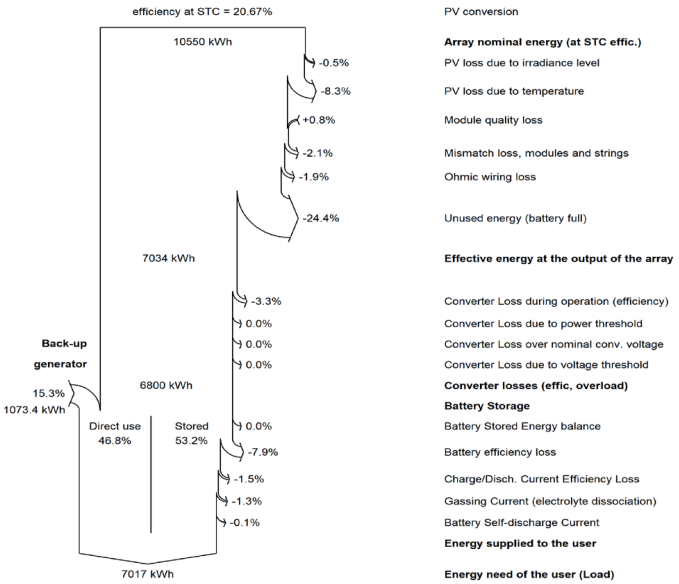


Fig. 10. PV system losses diagram

The installation of 100,000 rooftop PV solar systems reduces the $CO_2$ emissions to approximately 390,585 tons annually in case of completely generated by conventional power plants, and at least 480,720 tons when using common backup generators.

## D. Libyan Government's Benefits

According to the simulation results of proposed system, the annual installation of 100,000 systems will generate 601 GWh of solar energy, which will save the state of Libya an estimated of 132 million $ annually. It was frequently spent to generate the exact amount of electric power through traditional power plants. Therefore, based on fuel international prices, the state of Libya will effectively be able to reimburse roughly 132 million US Dollar within 39 months. In addition, Libyan government will get indirect gains such as, get banks involved on investment sector as well as refreshing labor market, activate the participation of private companies. The research centers and advisory institutions will share data collection and attempt to develop such new technology.

# X. The Proposal Implementation Approaches

- Preparing an electronic system, which operates via ship that has the owner information, and can be accessed by third party authorities. That could be done as following:

✓ The citizen or beneficiary, announcing to people who are willing to acquire the system through a link created for this purpose then they can register online. The costumer will be able to follow the installation procedures according to announced date and time.

✓ The company, which is the authorized public authority responsible for the supply, sale and guarantee the solar systems.

✓ The bank is responsible for financial procedures, clearing and financing if required.

✓ -Installation and connection (provided by private companies): represented by the installation teams of private companies.

✓ Inspection and supervision: Both are a duty of a third party who authorized and responsible for pre-inspection, verification of the systems installation. Accordingly, they are responsi-


Saleh Eshtaiwi, Mustafa Aburwais, Osama Elsanusi, Mustafa Elayeb, Mohamed Shetwan, The Impact of Residential Optimally Designed Rooftop PV System on Libya Power Shortage Case, Journal of Energy, vol. 71 Number 3 (2022), 3–9
https://doi.org/10.37798/2022713377

ble for training teams to study and analyze the operation data.

- ✓ Collection: the GECOL is responsible for verifying the payment of debts incurred by the costumer.
- ✓ The supporter (Libyan government): It should pay the price difference, whether in relation to the exchange rate or the subsidy rate.
- ✓ Follower (the third party): It is the entity responsible for managing the process through the electronic system and legal and spatial follow-up remotely.
    - Public announcement for project applying conditions for the solar systems, and inviting people who is willing to own one of those system referenced. the people who is willing to obtain those systems register through the announced link enter their information, including: a username and a password, to follow the procedures. Accordingly, they enter to waiting list and they obtain an indication number to follow-up with the procedure. Inspection teams communicate with cases that automatically appear on the side of their system, and set an appointment to visit the installation site. If the installation site is not valid (no enough space, shadow, or any other condition makes the site not valid for installation), the case will be removed from the waiting list and the system will send an apology letter to the costumer via phone. Once site is suitable for installation, the result is documented on the system to appear to the rest of the parties responsible in the process, hence a message will be sent to the customer to review the funding steps.
    - The case remains in the waiting list until the customer settles his debts with the GECOL.
    - Based on the result of the inspection and collection teams, the solar system is initially reserved within the company's list automatically then the process appears on the side of the bank's system and a message is sent to the costumer that he has an appointment at the bank.
    - The customer contacts his bank to complete the procedures for withholding the price of the system from his account, or requesting lending according to the financing methods provided by the bank.
    - The bank transfers half price of the solar system to the company's account, thus making the final reservation. Then, the case appears in the company's waiting list as well as installation teams. The claim is sent to the supporting party to transfer half of the subsidy value to the company's account, respectively.
    - The installation teams receive the solar systems and communicate with customers to complete the installation process according to the lists that appear to them in the electronic system. The installation team submit a report about the installation at the electronic system whenever they done their job.
    - The inspection team will follow up with the report who will be responsible of installation safety and observing the operation conditions as well as train the costumer dealing with the system.
    - The inspection team has to submit a report to the electronic system once they done with their job. Then, the bank and the supporting party have to pay the rest of the dept to the company's account which is going to pay the installation costs.
    - Finally, the company issues the manufacturer's warranty document for the solar system that starts at installation date of receipt and provides the after-sale provision services for a period not less than the warranty period.

## XI. Conclusion

This paper introduced three Scenario of PV rooftop systems appropriate for Libyan household's appliances. Models of typical Libyan homes appliances were considered. It ended up with a proposal of hybrid PV solar system that should be widely installed. Therefore, it can be summarized that system with a nominal capacity of 5.65 $kW_p$ and run to supply an annual energy estimated at 7.017 MWh, with a solar contribution rate of 84.7%, will clearly minimize the consequences of Libya power shortage. Since 100,000 PV systems are highly recommended to get it installed annually, it thus generates 601 GWh every year. Consequently, the project can simply reduce $CO_2$ emission by 390,585 ton yearly. Furthermore, it will aim to save 132 million US dollar every year which Libyan government afford to support GECOL with for burning fuel. The growing of PV systems creates power reserve which indirectly extend electric grid equipment lifespan. Therefore, the project will successfully strengthen the awareness of power grid independency. Nevertheless, the Tariff of 0.082 $/kWh should be certainly updated in terms of power saving and sustainability enhancement.

## References


[1] T. G. M. o. Generation, "Monthly Generation Report," GECOL, Tripoli 2022.

[2] A. N. Y. Al-Athram and others, "Report on applying PV systems on rooftops," GECOL, Tripoli, Libya 2017.

[3] S. Ben_Naseer and F. Gashout. Application of Roof-Top PV Solar Panels [Online]. Available: https://sec.leaboz.org.ly/

[4] S. Eshtaiwi, M. Aburwais, M. Elayeb, M. Abozaed, and M. Shetwan, "Rooftop PV systems as a solution to the electrical power shortage in Libya," *IET Conference Proceedings,* pp. 441-447Available: https://digitallibrary.theiet.org/content/conferences/0.1049/icp.2023.0033

[5] K. A. Glaisa, M. E. Elayeb, and M. A. Shetwan, "Potential of Hybrid System Powering School in Libya," *Energy Procedia,* vol. 57, pp. 1411-1420, 2014/01/01/ 2014.

[6] J. M. Takouleu. LIBYA: Irish AG Energy to build a 200 MWp solar power plant in Ghadames [Online]. Available: https://www.afrik21.africa/en/libya-irish-ag-energy-to-build-a-200-mwp-solar-power-plant-in-ghadames/

[7] T. G. M. o. Control, "Electricity Daily Load Profile - Public Electrical Grid," GECOL, Tripoli 2022.

[8] S. Al-Hashmi, M. Sharif, M. Elhaj, and M. Almrabet. The Future of Renewable Energy in Libya [Online]. Available: https://www.bulletin.zu.edu.ly/issue_n19_3/Contents/E_07.pdf

[9] V. SHAW. Trina Reveals 600 W Module [Online]. Available: https://www.pvmagazine.com/2020/07/20/trina-reveals-600-w-module/

[10] E. Yao, P. Samadi, V. W. S. Wong, and R. Schober, "Residential Demand Side Management Under High Penetration of Rooftop Photovoltaic Units," *IEEE Transactions on Smart Grid,* vol. 7, no. 3, pp. 1597-1608, 2016.

[11] M. J. E. Alam, K. M. Muttaqi, and D. Sutanto, "Mitigation of Rooftop Solar PV Impacts and Evening Peak Support by Managing Available Capacity of Distributed Energy Storage Systems," *IEEE Transactions on Power Systems,* vol. 28, no. 4, pp. 3874-3884, 2013.

[12] C. Prapanukool and S. Chaitusaney, "An appropriate battery capacity and operation schedule of battery energy storage system for PV Rooftop with net-metering scheme," in *2017 14th International Conference on Electrical Engineering/Electronics, Computer, Telecommunications and Information Technology (ECTI-CON)*, pp. 222-225, 2017

[13] Y. Song and B. Wang, "Survey on Reliability of Power Electronic Systems," *IEEE Transactions on Power Electronics,* vol. 28, no. 1, pp. 591-604, 2013.

[14] N. C. Sintamarean, F. Blaabjerg, H. Wang, F. Iannuzzo, and P. d. P. Rimmen, "Reliability Oriented Design Tool For the New Generation of Grid Connected PV-Inverters," *IEEE Transactions on Power Electronics,* vol. 30, no. 5, pp. 2635-2644, 2015.

[15] S. B. Kjaer, J. K. Pedersen, and F. Blaabjerg, "A review of single-phase grid-connected inverters for photovoltaic modules," *IEEE Transactions on Industry Applications,* vol. 41, no. 5, pp. 1292-1306, 2005.

Journal of Energy
VOLUME 71 Number 3 | 2022
journal homepage: http://journalofenergy.com/

# MAAP 4.07 Analysis of Long Term Containment Heat Removal after Reactor Vessel Failure (DEC-B) for Nuclear Power Plant Krško (NEK)

Robi Jalovec, Srđan Špalj

***Summary* — The paper presents the MAAP 4.07 analysis of containment heat removal after reactor vessel failure resulting from the initial Station Blackout (SBO) accident. The accident is analysed considering mitigation measures for heat removal from the containment using alternative equipment (Alternative Residual Heat Removal (ARHR) pump and heat exchanger (ARHX) and, also, Alternative Safety Injection (ASI) pump). The mitigation actions are taken according to NEK Severe Accident Mitigation Guidelines (SAMG). There are several possibilities to remove the heat from the containment once the reactor vessel fails and, for all of them, the necessary condition is to have the sufficient source of water (Residual Water Storage Tank (RWST), Alternative Boron Water Tank (ABWT) or other) and the appropriate heat exchanger available. Two options are presented within this paper: Injection to the Reactor Coolant System (RCS) using ASI pump and recirculation (sump to RCS) through ARHR system via ARHX, and Spraying the containment through Containment Spray (CI) system using ARHR pump and, then, recirculation (sump to spray) through CI and ARHR systems via ARHX. The results show that the containment heat removal can be done with either of analysed ways if the water is provided for recirculation (assumed containment level 3.9 m ~ 760 m³). However, with the fact that the reactor cavity is not flooded, the cooling using ASI will initially result in considerable containment pressure increase because the water is spilled through the RCS over the hot molten core debris. Therefore, it must be stated that the preferable way of containment pressure reduction, once the vessel has failed, is by using the containment spray. On the other hand, if RWST is not available, then the initial water delivery cannot be made from ABWT via CI system because this option does not exist. It shall also be pointed out that, if the active containment heat removal is started early enough, the Passive Containment Filtered Vent System (PCFVS) opening would be prevented and no fission products shall be released to environment.**

***Keywords* — station blackout (SBO), containment heat removal, design extension conditions (DEC), MAAP 4.07, Nuclear Power Plant Krško (NEK)**

(Corresponding author: Robi Jalovec)
Robi Jalovec and Srđan Špalj are with the Nuclear Power Plant Krško (NEK) Krško, Slovenia (e-mails: robi.jalovec@nek.si, srdjan.spalj@nek.si)

## I. Introduction

Following the lessons learned from the accident at the nuclear power plant Fukushima Daiichi in Japan and according to the Slovenian Nuclear Safety Administration (SNSA) Decree No.: 3570-11/2011/7 on September 1, 2011 [1] Nuclear Power Plant Krško (NEK) decided to take the necessary steps for upgrade of safety measures to prevent severe accidents and to improve the means to successfully mitigate their consequences.

The potential plant upgrades of existing structures, systems and components (SSC) and other measures and new systems that are important to provide nuclear safety during severe accidents are focused in the following areas:

1. AC power supply from external and internal sources,
2. Reactor core cooling with primary (injection to primary system) and secondary systems (reactor cooling through the steam generators),
3. Containment integrity at high temperature conditions, overpressure and high Hydrogen concentrations,
4. Controlled releases from the plant to the environment (less than 0.1 % of aerosols and particulates from core fission products),
5. Core cooling and control during severe accidents from the alternative control room and,
6. Alternative cooling of spent fuel pool.

One of the modifications that NEK has implemented is the installation of alternative RHR pump and alternative RHR heat exchanger (RCS and Containment Alternative Cooling). This modification, among the other already existing systems, serve for the purpose of reactor decay heat removal either from the RCS or from the containment once the core and RCS are severely damaged.

This paper presents the analysis of the NEK containment response following DEC-B ([2], [3]) accident considering mitigation measures for heat removal from the containment. DEC-B (Design Extension Condition B), as defined in IAEA SSR 2/1 [2] and WENRA RL [3], are those conditions that involve severe damage of the reactor core. Presented analysis is focused on containment heat removal after reactor vessel failure resulting from the initial SBO accident. It also addresses the containment cooling for the period before and after reactor vessel failure with the aim to prevent the operation of PCFV system.


Robi Jalovec, Srđan Špalj, MAAP 4.07 Analysis of Long Term Containment Heat Removal after Reactor Vessel Failure (DEC-B) for Nuclear Power Plant Krško (NEK), Journal of Energy, vol. 71 Number 3 (2022), 10–15
https://doi.org/10.37798/2022713418

The analyses were performed using MAAP 4.07 computer code. As a result, the methods of containment cooling are described with benefits and possible negative aspects.

## II. Methods – Background Information

### *A Modular Accident Analysis Program (MAAP) description*

The Modular Accident Analysis Program (MAAP) Version 4.0.7 is a computer code [4] that can simulate the response of light water reactor power plants, like NPP Krško, during severe accident sequences, including actions taken as part of accident management. The code quantitatively predicts the evolution of a severe accident starting from full power conditions given a set of system faults and initiating events through events such as core melt, reactor vessel failure, and containment failure. Furthermore, models are included to represent the actions that could stop the accident by in-vessel cooling, external cooling of the RPV or cooling the debris in containment (ex-vessel cooling).

MAAP4 treats the spectrum of physical processes that could occur during an accident including steam formation, core heatup, cladding oxidation and hydrogen evolution, vessel failure, core debris-concrete interactions, ignition of combustible gases, fluid (water and core debris) entrainment by high velocity gases, and fission product release, transport, and deposition. MAAP4 addresses all of the important engineered safety systems such as emergency core cooling, containment sprays, fan coolers, and power operated relief valves. In addition, MAAP allows operator interventions and incorporates these in a flexible manner, permitting the user to model operator behaviour in a general way. Specifically, the user models the operator influence by specifying a set of variable values and/or events which are the operator intervention conditions combined with associated operator actions.

MAAP is fast running code and most of the processes are modelled using ordinary differential equations without spatial dependency and phenomenological models were used. Such code is capable to predict correct overall behaviour of the system, but local conditions are approximate due to both used models and rather crude subdivision (nodalization) of the object. Different parts of the model, including containment, have recommended ways how to prepare subdivision dependent on the type of the plant.

### *B NEK MAAP model*

The plant itself, its systems and regions (nodalization) is modelled through parameter file, described below. The event sequence is externally controlled through input decks. A structured (symbolic) language can be used to model operator actions, control output of variables or model the deficiencies in the engineered safety features.

The MAAP parameter file [5] primarily represents a database describing Krško nuclear power plant in some detail. It focuses on reactor coolant system, engineered safeguards and containment. The second important role of the parameter file is to supply control parameters, user and code controlled messages, print file parameters aimed at accurate simulation of plant operation.

In general, the Krško parameter file can be broken into six major categories.

1) Control Parameters

2) Reactor Core Parameters

3) Primary System/Safety System Parameters

4) Containment/Auxiliary Building Parameters

5) Specific Plant Feature Parameters

6) Event Code Parameters

*Control Parameters* describe input parameters for: model selection and program control; key phenomenological models; defining the thermo-physical properties of concrete; timing control; integration control; selection of variables to be written to data files for plotting; selection of variables to be written to the tabular and/or log files.

*Reactor Core Parameters* describe input parameters for reactor core setup and fission products.

*Primary System/Safety System Parameters* describe input parameters for: initial conditions; the reactor pressure vessel geometry and setup; pressurizer geometry and setup; steam generator geometry and setup; the engineered safeguard safety systems; the generalized engineered safety system pump properties.

*Containment/Auxiliary Building Parameters* describe input parameters to: assign the compartment indices; assign elevations for primary system - containment interfaces; set up the containment/auxiliary building compartment geometry; set up the containment/auxiliary building flow paths between compartments; the corium debris pools in the containment; heat sink thermal properties used for distributed and lumped heat sinks; distributed heat sinks such as walls and floors; lumped heat sinks such as structural materials; modeling the containment outer wall stress/strain.

NEK containment building is divided into ten compartments: Reactor Cavity (1), Lower (2), Upper (3), Annular (4), Steam Generators (5 & 6), Spherical (7), Sump (9), Pressurizer (10) Compartments. The MAAP4 recommendation is to represent the free standing steel containment wall and the shield building wall as two distinct walls with gap between them modeled as a compartment, Annulus (8).

Figure 1 shows MAAP nodalization of primary, secondary and Emergency Core Cooling System (ECCS) for NPP Krško. Figure 2 presents containment nodalization scheme for NPP Krško used in MAAP code.

For the transient analysis the input file shall also be developed. Input file defines the sequence of transient: accident initiators, operator actions, time/sequence control, changes to parameter file, file setup, output specification.


Robi Jalovec, Srđan Špalj, MAAP 4.07 Analysis of Long Term Containment Heat Removal after Reactor Vessel Failure (DEC-B) for Nuclear Power Plant Krško (NEK), Journal of Energy, vol. 71 Number 3 (2022), 10–15
https://doi.org/10.37798/2022713418

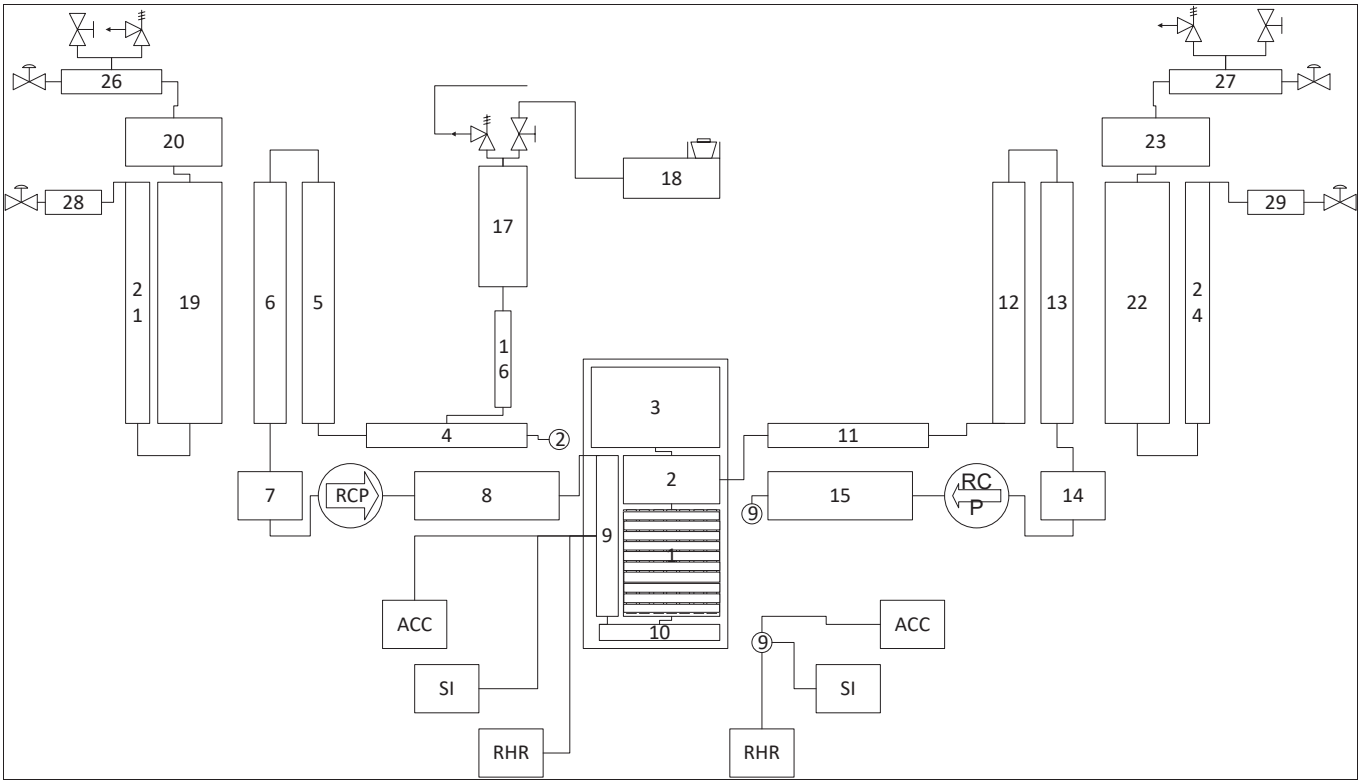


Fig. 1. NPP Krško nodalization of primary system, secondary system and ECCS

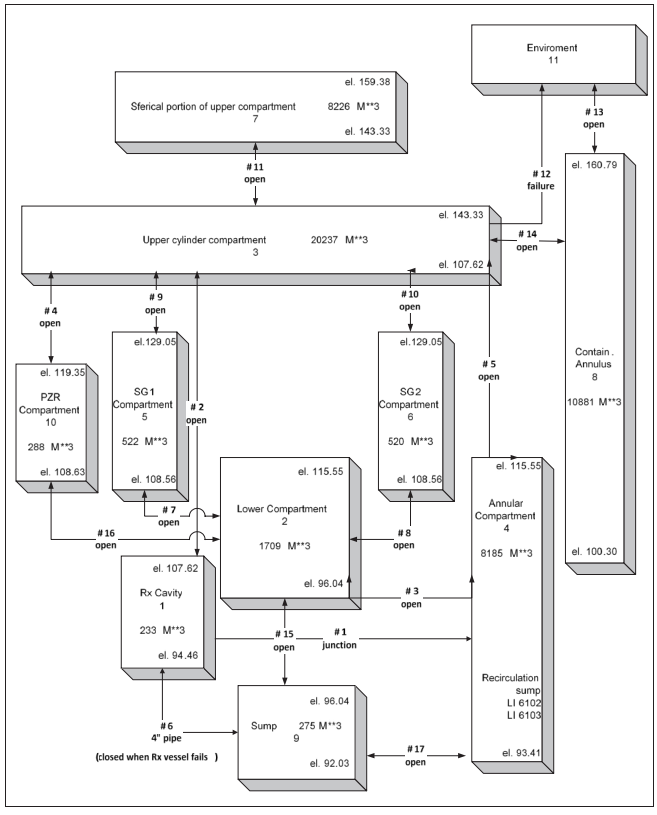


Fig. 2. NPP Krško containment nodalization scheme

## III Analysis, Evaluation, Calculation

### *A. Transient Description*

The analyses are focused on long term containment heat removal after reactor vessel failure (DEC-B) resulting from the initial SBO accident. SBO scenario involves a loss of offsite power, failure of the redundant emergency diesel generators, failure of AC power restoration and the eventual degradation of the RCP seals resulting in a long-term loss of coolant. It is assumed that AC power exists only on the AC buses powered by inverters connected to the station batteries. Loss of all AC power results in unavailability of all normal electrical equipment and most of the safety electrical equipment. The only possible corrective actions are reactor trip and residual heat removal using steam generator (SG) safety and relief valves and turbine (steam) driven auxiliary feedwater (TD-AFW) pump if available. The loss of coolant increases the probability of core melt. The potential locations for coolant losses are primary coolant pump seals, letdown relief valve and pressurizer valves.

Following the loss of all AC power the RCP seals would lose their cooling support systems and would experience a serious thermal transient. This conservative assumption remains regardless the fact that the High-Temperature RCP seals were installed recently. The charging and letdown system would not be available so that there would be no make-up water supply to the seals. Component cooling water to the RCP thermal barrier heat exchanger would also be unavailable. Leakage of RCS fluid through the RCP seals would be a small LOCA without makeup capability which will lead to core uncovery and heat-up, and, possibly, to a core damage. Depending of the availability of heat sink and the RCP seal leakage rate, the SBO transient can result in vessel and containment failure.


Robi Jalovec, Srđan Špalj, MAAP 4.07 Analysis of Long Term Containment Heat Removal after Reactor Vessel Failure (DEC-B) for Nuclear Power Plant Krško (NEK), Journal of Energy, vol. 71 Number 3 (2022), 10–15
https://doi.org/10.37798/2022713418

### B. Initial and Boundary Conditions for Long Term Station Blackout

The following is the scenario of SBO accident:

- loss of offsite power,
- failure of the emergency diesel generators,
- failure of AC power restoration,
- degradation of the RCP seals resulting in a long-term loss of coolant. The seal leakage rate is 21 gpm/RCP,
- letdown line isolation and, consequently, opening of letdown relief valve if RCS pressure is greater than 42.2 kp/cm².

The main assumptions for the SBO analysis are:

- reactor trip from 100 % power,
- RCPs trip,
- turbine trip,
- main steam line isolation (MSIVs trip),
- feedwater closure (trip of MFW and motor-driven AFW pumps),
- RCPs seal flow not available,
- steam dump not available,
- charging and letdown flow not available,
- high pressure injection system (HPIS) not available,
- low pressure injection system (LPIS) not available,
- pressurizer proportional and backup heaters not available,
- SG Power Operated Relief Valves (PORVs) available
- TD AF pump not available (total loss of heat sink is assumed)
- Containment spray not available
- Containment fan cooler not available
-

No operator actions are assumed prior to the core damage and are focused on mitigation of consequences in order to prevent the containment failure. The following cases were analysed with respect to the operator actions:

1. Mitigation after vessel failure using CI and ARHR recirculation
2. Mitigation after vessel failure using ASI injection and ARHR recirculation

### C. Analysed cases

There are several possibilities to remove the heat from the containment once the reactor vessel fails and, for all of them, the necessary condition is to have the sufficient source of water (RWST, ABWT or other) and the appropriate heat exchanger (HX) available. These possibilities are:

1. Recirculation from sump to reactor coolant system (RCS) through RHR system (either standard or alternative path) using standard or alternative RHR HX. For this purpose, it is necessary to deliver water into containment in either of the achievable ways:
    a. Injection to RCS using alternative SI (ASI) pump or another available pump
    b. Containment spray (CI) system
    c. RWST gravity drain
    d. Injection to containment via dedicated penetration (RH-1043-0460).
    e. Fire Protection (FP) system using Severe Accident Management Equipment (AE), what is already foreseen as one of the Severe Accident Management action.
2. Recirculation from sump to Containment Spray (CI) via alternative RHR system (ARHR) and alternative RHR heat exchanger (ARHR HX). It is also necessary to deliver water to the containment at the same way as described above.
3. Recirculation through ARHR HX via penetration RH-1043-0460. The prerequisite for this action is to have sufficient amount of water to enter the reactor cavity.
4. Use of containment fan coolers (RCFC). This is DBA equipment which is not considered to function under DEC, therefore, this option is not relevant.

The analyses presented here were done for containment heat removal considering options 1 (RCS – (A)RHR HX) and 2 (CI – ARHR HX) above. The water was delivered from ABWT or RWST via ASI and CI pump, since other options (c, d and e above) for water delivery are impossible or rather complicated to model within MAAP computer code. The actual characteristics of alternative RHR heat exchanger and alternative RHR pump have been incorporated into MAAP model. The maximum expected ASI flowrate is approximately 285 m³/h (the maximum standard SI pump flow rate is ~160 m³/h). In the MAAP model the normal spray line-up is used and the characteristics of spray pump is changed to the characteristics of ARHR pump.

The start of recirculation is assumed at containment water level 3.9 m (measured with sump level indicators LI 6102 and LI 6103) which is SAMG set-point and the corresponding volume is around 760 m³. To protect the containment vessel against hydrogen burn it is necessary to limit the heat removal so the mitigation action is stopped at 1.5 kp/cm² and the heat removal is again started at 3.15 kp/cm², (SAMG set-point [6]). This action remained for 2 days after the recirculation has started (arbitrary) regardless low hydrogen concentration. After that period the set-points were changed to -0.1 kp/cm² to 0.28 kp/cm² (all mention set-pints are gauge pressure).

For each of the evaluated options (1 and 2 above) 3 different cases, with respect to the mitigation start (regardless of the required containment pressure set-point), was analysed:

- mitigation starts at 8 h,
- mitigation starts at 24 h (before the first PCFVS venting),
- mitigation starts at 40 h (after the first PCFVS Venting).

### D. Containment heat removal using containment spray (CI) aligned to ARHR

Figure 3 to Figure 5 present the comparison of the accidents for different start of containment heat removal using containment spray (CI). It was assumed that the water is initially delivered from RWST using standard CI pump and then recirculated by ARHR pump via ARHR HX, as described above. If RWST is not available, then the initial water delivery cannot be made from ABWT or other tank via CI system because these options do not exist.

From the figures below, it can be clearly seen that the heat removal is successful. The pressure reduction starts immediately after CI initiation. The increase of the pressure, that can be noticed (Figure 3) for all three cases, starts around 2.5 hours after beginning of spraying and pressure reduction. It is the result of water evaporating after spilling into the reactor cavity though ventilation duct over molten core debris. This evaporation results in the second PCFVS opening (Figure 3 and Figure 4), for the case when cooling starts at 40 h, when pressure rises above set-point of 4.9 bar abs. The total release of noble gases is around 40% (Figure 4). For other two cases the cooling is effective and there is no PCFVS opening. Over the longer time scale the pressure behaviour is dictated by the operator actions required in SAMGs [6], as described in the above (heat removal cycling between 1.5 kp/cm² and 3.15 kp/cm², and changed to -0.1 kp/cm² to 0.28 kp/cm² two days after recirculation has started). The hydrogen production during Molten Core


Robi Jalovec, Srđan Špalj, MAAP 4.07 Analysis of Long Term Containment Heat Removal after Reactor Vessel Failure (DEC-B) for Nuclear Power Plant Krško (NEK), Journal of Energy, vol. 71 Number 3 (2022), 10–15
https://doi.org/10.37798/2022713418

Concrete Interaction (MCCI) is quite extensive (Figure 5) except for the case when spraying starts at 8 hours and the water is spilled over the ventilation duct before substantial MCCI begins. It shall be mentioned that, for all cases, the MAAP code predicts that the MCCI is stopped immediately once the water is spilled over the molten core debris.

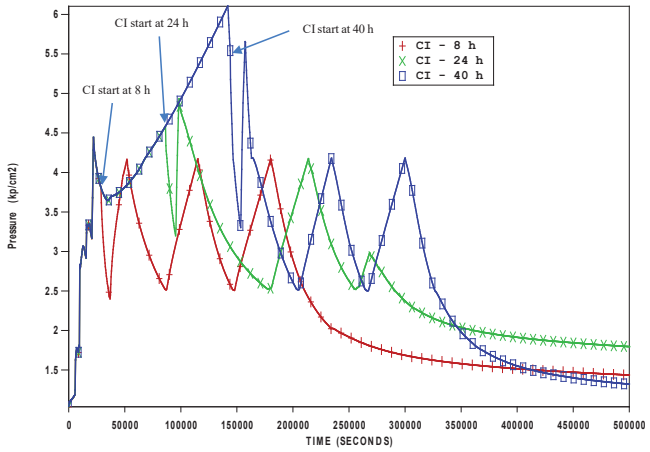


Fig. 3 Containment pressure – cooling with CI + ARHR

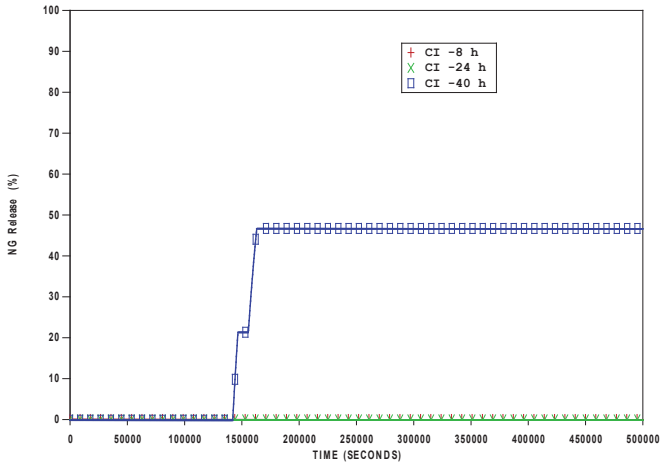


Fig. 4 Noble gases release from containment - cooling with CI + ARHR

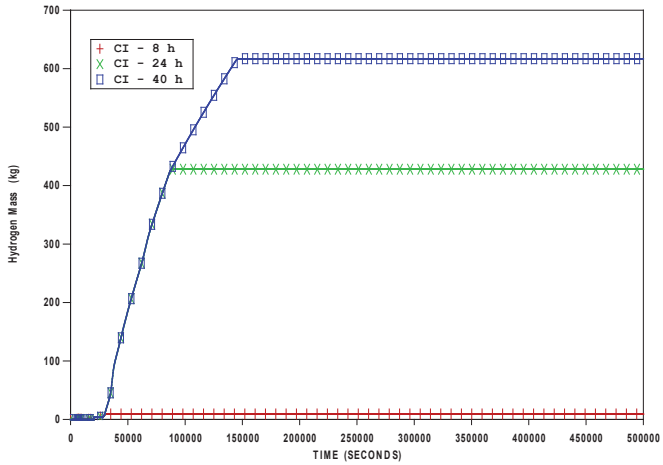


Fig. 5: Hydrogen produced during MCCI – cooling with CI + ARHR

## *E. Containment heat removal using ASI to RCS and ARHR recirculation*

There is significant difference between heat removal using ASI injected to RCS, then recirculated via ARHR, and the cases above (CI + ARHR). This is evident from the high pressure peaks in the Figure 6 below. These peaks are caused by extensive evaporation when the water spills over the hot molten core debris after it is injected to the RCS and exits through the failed reactor vessel. The capacity of the PCFV system is not sufficient (limited by 4" diameter orifice) to prevent pressure rise above 6 bar abs. The containment pressure increases far above this point, even over 7 bar abs, highly exceeding 5% failure probability at containment fragility curve what is required in the design of PCFV system. Only for the earliest injection (8 hours) the pressure increase is not challenging, and there is no PCFVS opening. For other two cases the PCFVS opening results in the release of noble gases below 40 % (case 24 h) and around 60 % (case 40 h). Hydrogen produced during the MCCI (Figure 8) is comparable to the case with containment spray initiation, even slightly below due to the earlier core debris flooding. Similarly, as for the previous case, on the long time scale the pressure behaviour is dictated by the operator actions required in SAMGs.

The comparison to the case with CI initiation for start of heat removal at 24 hours (Figure 9) shows the clear indication of pressure differences described above. Therefore, it must be stated that the preferable way of containment pressure reduction, once the vessel has failed, is by using of containment spray. The Fire Protection (FP) sprays for reactor coolant pumps can also be used for this purpose. Using of RCS injection shall be avoided if enough water is not assured in the reactor cavity to cover the core debris and/or the containment pressure is already high.

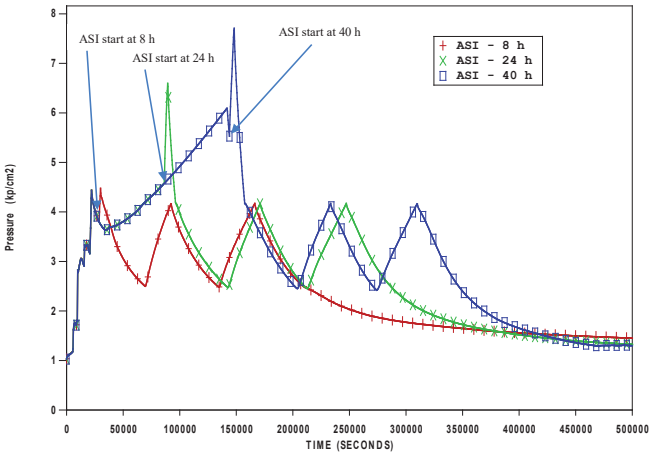


Fig. 6. Containment pressure – cooling with ASI + ARHR

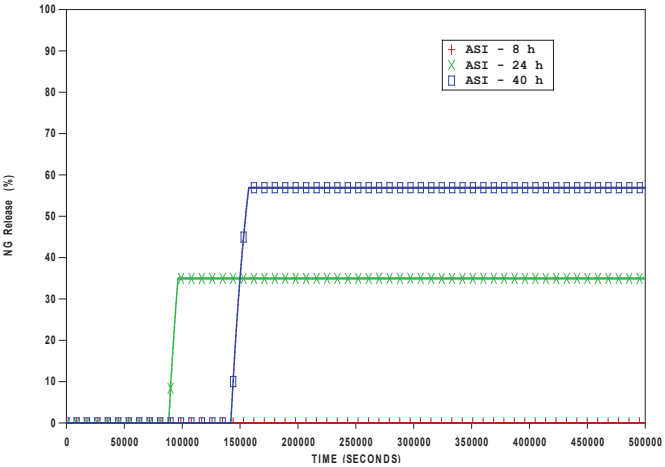


Fig. 7. Noble gases release from containment – cooling with ASI + ARHR


Robi Jalovec, Srđan Špalj, MAAP 4.07 Analysis of Long Term Containment Heat Removal after Reactor Vessel Failure (DEC-B) for Nuclear Power Plant Krško (NEK), Journal of Energy, vol. 71 Number 3 (2022), 10–15
https://doi.org/10.37798/2022713418

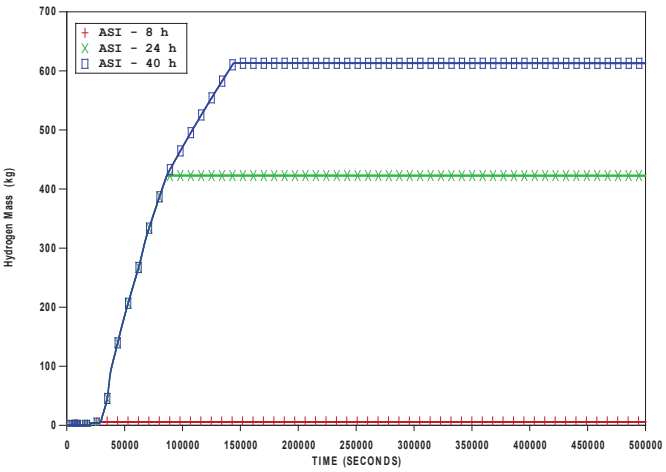


Fig. 8. Hydrogen produced during MCCI – cooling with ASI + ARHR

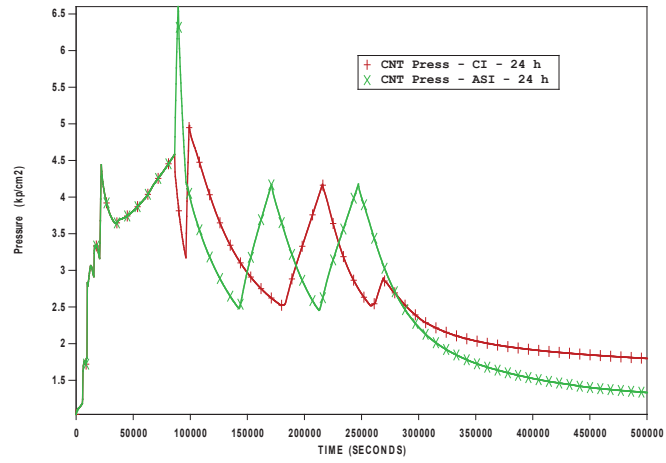


Fig. 9. Containment pressure, cooling start at 24 h, comparison for cooling with CI and ASI

## IV. Conclusion

This paper presented the analyses of long-term containment heat removal after reactor vessel failure (DEC-B) resulting from the initial SBO accident. It also addresses the containment cooling for the period before and after reactor vessel failure with the aim to prevent the operation of PCFV system. The analyses considered modification within NEK Safety Upgrade Project - installation of alternative RHR pump and alternative RHR heat exchanger.

The containment heat removal was analysed assuming that ARHR pump and ARHR HX, and also ASI pump, have the actual characteristics as implemented in the plant modifications. It shall be pointed out that cooling can be done with either of analysed ways - ASI, ARHR pump and ARHR HX or CI, ARHR pump and ARHR HX if the water is provided for recirculation (assumed 3.9 m ~ 760 m$^3$) either from RWST, ABWT or any other available source. However, the cooling using ASI will initially result in significant containment pressure increase (over PCFVS opening set-point) because the water is spilled through the RCS over the molten core. Therefore, it must be stated that the preferable way of containment pressure reduction, once the vessel has failed, is by using of containment spray (CI). On the other hand, if RWST is not available, then the initial water delivery cannot be made from ABWT or other tank via CI system because these options are not foreseen. The Fire Protection (FP) sprays for reactor coolant pumps can also be used for this purpose. Using of RCS injection shall be avoided if enough water is not assured in the reactor cavity to cover the core debris and/or the containment pressure is already high. It shall be also stated that if the active containment heat removal is started early enough the PCFVS opening would be prevented and no fission products shall be released to environment.

## References

[1] SNSA Decree No.: 3570-II/2011/7, "Odločba o izvedbi modernizacije varnostnih rešitev za preprečevanje težkih nesreč in blažitev njihovih posledic (SNSA Decree on Implementation of modernization of safety solutions for prevention of severe accidents and mitigation of their consequences)", September 2011.

[2] IAEA Safety Standard, Safety of Nuclear Power Plants: Design – Specific Safety Requirement, No. SSR-2/1, 2012

[3] WENRA SAFETY REFERENCE LEVELS FOR EXISTING REACTORS, Update in relation to lessons learned from TEPCO Fukushima Dai-Ichi accident, September 2014.

[4] MAAP 4.0.7 Users Manual, Fauske and Associates

[5] NEK ESD-TR-02/00, rev.0, NEK MAAP4 Parameter File Notebook

[6] SAMG-17, Severe Accident Management Guidelines, 2019

[7] NEK ESD-TR-18/15, Analysis of Containment Cooling During and After DEC-B Accidents, rev. 2, 2019.

[8] NEK ESD-TR-09/11, NPP Krško Analysis of Potential Safety Improvements, Rev. 0, January 2011;

[9] NEK ESD-TR-05/11, rev.1, Station Blackout Analyses as a Support for the NPP Krško STORE Actions and the Strategies Addressed in B.5.b Phase 2 & 3 Submittal Guideline

[10] WENX-12-05 / STR-NEK-11-18: "Krško Passive Containment Filtered, Pressure Relief Ventilation System Partial Conceptual Design Package", Rev. 1, Westinghouse.

[11] WENX-12-06: "Krško MAAP Analysis to Support Development of Partial Conceptual Design Package for Containment Severe Accident Hydrogen Control and Filtered Vent", Rev 1, Westinghouse.

[12] WENX-12-27: "Sizing of Aerosol and Iodine Filters of the Passive Containment Filtered Vent System for NPP Krško", Rev. 1, 2013, Westinghouse

[13] WENX-12-33: "Sizing of Passive Autocatalytic Recombiners", Rev. 1, 2013, Westinghouse

[14] NEK ESD-TR-25/13, rev.0, Estimation of Fission Products Release to Environment for Station Blackout (SBO) Accident Following Passive Containment Filtered Vent (PCFV) System Installation, December 2013.

[15] NEK ESD-TR-08/14: "NPP Krško MAAP Analysis of Station Blackout (SBO) Accident Following Passive Containment Filtered Vent (PCFV) System and Passive Autocatalytic Recombiners (PAR) Installation", Rev. 0, 2014.

[16] NEK Safety Upgrade Project Design Inputs and Interfaces, Rev. 8, 2016.

Journal of Energy

VOLUME 71 Number 3 | 2022

journal homepage: http://journalofenergy.com/

# Electric Vehicle Charging Infrastructure in Croatia – First-Hand Experiences and Recommendations for Future Development

Hrvoje Pandžić, Bojan Franc, Stjepan Stipetić, Franko Pandžić, Matko Mesar, Marija Miletić, Sara Jovanović

***Summary* — One of the most serious obstacles to massive deployment of electric vehicles is insufficient and cumbersome charging infrastructure. Both the number of charging points and their power capacity are often insufficient. On top of that, this new technology often suffers from many issues related to insufficient testing, immaturity and irregular handling. This paper summarizes the issues with the electric vehicle charging infrastructure and describes first-hand experiences with long-range electric vehicle trips originating from Zagreb, Croatia, during 2022. Issues with the charging points locations, power and availability are assessed. Based on these experiences, the paper provides some thoughts on the possible directions of the further development of the electric vehicle charging infrastructure in Croatia.**

***Keywords* — electric vehicles, charging infrastructure, range anxiety**

## 1. Introduction And Literature Review

Even though the very first electric vehicles appeared already in the nineteenth century, poor battery performance, large weight and short range made them inferior to the internal-combustion-powered vehicles throughout the twentieth century. However, the development of high-capacity and highly efficient lithium-ion battery cells (see [1]), increased concern for the environment and introduction of renewable energy sources (see [2]), and global digitalization of personal transportation systems set battery-powered electric vehicles as the main pillar of the future personal vehicle transport. A survey among early adopters of electric vehicles found that the two main reasons for purchasing an electric vehicle are care for the environment and vehicle design [3]. While studies such as [4] showed that investments in electric vehicles in Croatia are profitable, electric vehicle (EV) adoption is minimal. The shares of EVs are going to rise, fueled by the abovementioned reasons, but also by European legislation promoting cleaner transportation sector. For example, the European Parliament has in early 2023 approved the law banning new sales of diesel vehicles from 2035 [5].

(Corresponding author: Hrvoje Pandžić)

Hrvoje Pandžić, Bojan Franc, Stjepan Stipetić, Franko Pandžić, Matko Mesar, Marija Miletić and Sara Jovanović are with the University of Zagreb Faculty of Electrical Engineering and Computing (FER)

Zagreb, Croatia (e-mails: hrvoje.pandzic@fer.hr, bojan.franc@fer.hr, stjepan.stipetic@fer.hr, franko.pandzic@fer.hr, matko.mesar@fer.hr, marija.miletic@fer.hr, sara.jovanovic@fer.hr)

This work was supported by the Croatian Science Foundation and the European Union through the European Social ´Fund under project Flexibility of Converter-based Microgrids – FLEXIBASE (PZS-2019-02-7747).

The charging infrastructure, which imposes a massive impact on the electric grid, does not develop as rapidly and coherently as the electric vehicle owners would prefer. Although only around 5% of all charging occasions took place at public charging stations [6], long trips require charging points at relevant locations and are important to the users even if such trips occur only a few times per year. The charging infrastructure was promoted through several legal documents from the Clean Energy Package, such as the Energy performance in buildings directive [7] and Renewable energy directive [8]. The reasons for insufficient public charging infrastructure are both the high investment cost and the high operating costs, especially for high-power charging stations. In most countries, industrial loads, besides the consumed energy and network fees, need to pay for peak load on either monthly or annual basis (see [9] for details). Thus, underutilized charging points are not profitable, and there is still an insufficient number of EV owners to justify such investment. However, Croatia is a tourist country and an increasing number of visitors own an EV. For this reason, development of the EV charging infrastructure supersedes the national transportation needs.

The authors in [10] performed a survey during 2018 on the charging infrastructure in the city of Stockholm. The survey aimed at providing responses on who, how and where uses this infrastructure and at collecting user experiences. The authors listed five main challenges identified from the survey:

1. Better control system for parked cars;
2. Improve information (charger types, signs, payment);
3. Increase number of public charging stations;
4. Integrate payment systems;
5. Charger maintenance and monitoring.

The first challenge mainly refers to the fact that a vehicle can be parked at a charging station without charging. This usually happens after the charging session has finished, but the owner did not move their vehicle. Today this issue is resolved in at least two ways. The first one is charging the customers per minute spent at the charger, instead of the charged energy. The second one is charging per minute after the charging session had finished. In this case the customers are still charged per kWh, which is followed by per-minute cost upon the vehicle getting fully charged.

Regarding the second challenge, necessity for better information sharing and education was recognized by authors in [11] who analyzed the challenges for adopting EVs in Croatia. However, a big part of the issue has already been solved. Primarily, the charger types are standardized. Electric vehicles in Europe predominantly



Hrvoje Pandžić, Bojan Franc, Stjepan Stipetić, Franko Pandžić, Matko Mesar, Marija Miletić, Sara Jovanović, Electric Vehicle Charging Infrastructure in Croatia – First-Hand Experiences and Recommendations for Future Development, Journal of Energy, vol. 71 Number 3 (2022), 16–23
https://doi.org/10.37798/2022713414

use Type 2 for AC charging and CCS 2 for DC charging, although there are some vehicles still using CHAdeMO, e.g. Nissan Leaf. On the other hand, the charging stations are highly standardized. The most common 50 kW charging stations in Europe include all three chargers, i.e. Type 2, CCS2 and CHAdeMO. The road signs for charging stations have been standardized as well and there is no problem with recognizing them. However, the gas stations, at least the ones in Croatia, still do not offer a specialized sign for EV charging stations being available at their premises. This makes EV charging less exposed than gasoline, diesel and liquefied petroleum gas (LPG), all of which have a designated sign at the gas stations. Furthermore, the information available online are insufficient and unreliable.

The third issue will remain problematic for the foreseeable future as the number of chargers and their charging speed highly depend on the number of users and their willingness to pay extra for high-speed charging. The authors in [12] assessed the attitudes toward electromobility in Croatia. They found that neither policies aimed at encouraging electromobility, nor the deployed infrastructure have had positive impact on the attitudes toward electric vehicles. A study on a road and a power system segment in Croatia presented in [13] showed that coordination between the transport system planners and power system planners is central to high adoption of electromobility. The authors in [11] emphasize the problem of uneven distribution of charging stations for both domestic adoption of EVs and the highway congestion management during the tourist season.

Payment systems indeed present deep waters for end users. There are numerous applications, usually focused on one country or region in Europe at best. When customer faces a new charging provider, usually it is required to scan a 2D bar code and input credit card data to start charging. This is inconvenient and has other disadvantages, e.g. trying to obtain a company receipt.

Regarding the final issues related to charging maintenance and monitoring, users report often issues with starting the charging process. In this case, calling a telephone number listed at the charging point can solve the issue. However, the unreliable maintenance schedules are still a problem, as are the unavailable call services.

According to [14], range anxiety risk is identified as the second most critical risk for an uptake of electric vehicles with high probability and high impact. Furthermore, the author of [15] states that the public EV charging infrastructure has both the functional and the psychological purpose. Density and reliability of public charging infrastructure increases consumer confidence and reduces range anxiety. The author of [15] also emphasizes that the underutilization of public charging infrastructure should not be considered an "adoption failure". Until novel schemes such as charge sharing presented in [16] take hold, charging infrastructure is the main bottleneck for long-distance EV travel. Lack of such infrastructure can be attributed to very high investment and operational costs. On top of the physical investment at the premises, the installation of EV charging infrastructure also contains connection costs, which are not negligible in most countries. During operation, the EV charging infrastructure operator is not subject only to the energy costs toward its supplier but also to the peak power costs toward the system operators. When having only a small amount of energy supplied to the EVs, these high peak power costs have a strong impact on the per-kWh energy cost.

The main goal of this study is to present specific experiences in taking long EV trips originating from Zagreb, Croatia. By summing the number of leading EV charging providers, Croatia in 2022 offers over 600 public charging locations with over 1.000 charging points. We decided to test some of them and describe our experiences in using the available public charging infrastructure. As all of us are users of conventional vehicles, i.e. petrol- and diesel-powered, this study provides indicators on the chance of adopting new driving and charging patterns and expectations.

## II. Trip Experiences

### A. Description

We conducted four different trips throughout the year 2022 (see Table I). A map of the trips can be found at [17]. All the trips were taken using Hyundai Ioniq 5 rear-wheel drive, with a 72,6 kWh battery, 160 kW and ULTRA, i.e. the most advanced, equipment package. The producer claimed autonomous range of 481 km, which is not attainable when driving at high speed on highways.

Table I

The Trips Taken in Hyundai Ioniq 5

| Trip | Date | One-way distance |
|---|---|---|
| Zagreb – Vienna | Tuesday, June 21 2022 | 360 km |
| Zagreb – Šibenik | Tuesday, June 28 2022 | 340 km |
| Zagreb – Voštane | Tuesday, July 5 2022 | 430 km |
| Zagreb – Dubrovnik | Sunday, November 6 2022 | 650 km |

The goal was to test various aspects of e-mobility in Croatia, such as: number of charging stations in rural area, availability, installed power capacity, charging speeds, wait times, travel comfort, travel speed and EV vs fuel car travel times.

## III. Trips

### A. Zagreb – Vienna

The trip started on Tuesday, June 21, 2022 at 11 am with a fully charged vehicle. Since the distance to Vienna is just under 400 km, the plan was to charge the vehicle before arriving to Vienna. The location for charging was the shopping mall City West in Graz. The vehicle was charged on a 50 kW CCS2 charger operated by Smartics (the reserved amount of money on the credit card was one hundred euros, which was consolidated few days later). The session lasted for an hour and six minutes, which resulted in charging of 35 kWh for 30 Eur. The trip to Vienna was smooth and the final state of charge was 42%. Since this is lower than half of the battery capacity, it was assumed that two charging sessions will be needed on the way back and that the battery will not last to Graz to use the same charger.

The trip back to Zagreb started on Thursday, June 23, around 17 h. After a cumbersome search, an ultra-high-speed 320 kW charging station was identified at Porsche Zentrum Wien-Liesing (address Ketzergasse 120, Vienna), which was not on the way and caused us a detour. To find this charging station we used the Monta app. First try of the charger activation did not work as an error was reported just prior to charging. The vehicle was moved to the other charger, which worked well. We charged 38 kWh for 15.81 Eur. The session lasted 17:25 min. Maximum charging power was 220 kW, but most of the session the power was in between 120 and 148 kW. The table below indicates the reduction in state of charge after charging above 80%. The charging process was cancelled at 89% state of charge, where the charging station reported that additional 14 minutes were expected to reach the 100% state of charge. This ultra-high-speed charging station is located at a secluded location and there was literally nothing to do during the charging process besides admiring the design and the speed of charging.


Hrvoje Pandžić, Bojan Franc, Stjepan Stipetić, Franko Pandžić, Matko Mesar, Marija Miletić, Sara Jovanović, Electric Vehicle Charging Infrastructure in Croatia – First-Hand Experiences and Recommendations for Future Development, Journal of Energy, vol. 71 Number 3 (2022), 16–23
https://doi.org/10.37798/2022713414

TABLE II

REDUCTION OF THE CHARGING POWER AT THE PORSCHE ZENTRUM WIEN-LIESING CHARGING STATION

| State of charge | Charging power |
|---|---|
| 82% | 101 kW |
| 83% | 87 kW |
| 84% | 83 kW |
| 85% | 74 kW |
| 86% | 72 kW |
| 87% | 67 kW |
| 89% | 55 kW |


Fig. 1 Porsche Zentrum Wien-Liesing charging station

After charging to 89%, we went to the shopping mall Westfield Shopping City Sud, only few km away from the Porsche Zentrum Wien-Liesing. The idea was to take advantage of this and slow-charge the vehicle to 100%. Even though Westfield Shopping City Sud is a huge shopping mall, we were only able to find Type 2 charging point with an additional regular shuko plug. Since we did not have a charging cable, we used shuko plug at 3.3 kW. The reserved amount was 20 Eur, however, no cost was claimed in the end. The charging experience at the Westfield Shopping City Sud was by far the worst throughout the trip.

Since we did not have sufficient charge to reach Zagreb, we performed one last charging session at Ionity station at Pesnica pri Mariboru in Slovenia. We used Monta to perform charging at maximum power 220 kW. At 59% state of charge, the charging power was 143 kW, while at 64% state of charge the power was 169 kW. This made us believe that the charging point altered the charging power itself. 39 kWh were charged within 12 minutes. The experience was very nice, which is further spurred by an unprocessed payment, second and final one on the trip.

Overall, the trip was pleasant. Although it took a bit of planning, we did not make many detours and most of the time felt confident about the vehicle's range. The largest disappointment was very basic charging infrastructure at the Westfield Shopping City Sud, while the most convenient charging session was the one in Slovenia.

### *B. Zagreb – Šibenik*

The trip to Šibenik began at about 6 a.m. on Tuesday, June 28th, 2022. The vehicle had been fully charged the night before at the charging station of FER. The stated range of the vehicle was 330 km when switched on, and the distance between FER and the site in Šibenik is 340 km. Therefore, we decided to charge the vehicle at the fast-charging station at INA station - Zir zapad - Mogorić 250. We arrived at the Zir station with about 20% SoC, connected the fast charger and started charging through the ELEN application. The charging process started with a power of 161 kW, continued with a power of 150 kW up to 80 % charge, and ended with a gradually decreasing power up to 95% battery charge. There was an issue with interrupting the charge as I received a mobile phone call during the charge: the ELEN app froze and indicated that the charge was complete, which was not true as it was continuing. Of course, the charging should not be interrupted by disconnecting the charging cable, and we did not want to activate the "safety mushroom", so we called the help-desk telephone number indicated on the charger, explained the situation, and they finished the charging remotely. Soon we received a receipt in the application. A total of 57.96 kWh was consumed at a cost of HRK 4.38/kWh + VAT 13%. The final cost was 286.85 HRK. Recharging took 28:18 minutes, which was not a significant amount of time, nor did it affect the comfort of the trip, as it is a normal break taken during trips in a conventional car to refuel or for the driver to rest. The feeling was compounded by the fact that we were the first in line to recharge, even though there is only one fast charger. We reached Šibenik with a remaining charge of 55%.

The return trip started at 15:30 from Šibenik and we arrived at the INA gas station - ZIR istok - Mogorić 251 with 13% charge. On this side of the highway there are only slow chargers, and the charging was performed with a power of 48.5 kW. Although we were the first in line and there were other non-occupied chargers, charging with a slow charger on the highway is a bad and slow experience. Charging took 1 hour and 9 minutes, and we intentionally exceeded the charging time of 60 minutes to still have enough power for the trip to Zagreb. We charged 53.31 kWh for 69 minutes at a cost of HRK 3.10 + VAT 13%. The final electricity cost was 186.73 HRK, with an additional penalty for overcharging for 9.8

| stavka | količina | cijena kn | popust kn | stopa PDV | iznos kn |
|---|---|---|---|---|---|
| isporučena električna energija punionica 50 kW dan | 53,3060 kWh | 3,10 | | 13,00 % | 186,73 |
| prekoračenje dozvoljenog trajanja punjenja | 9,8333 min | 0,80 | | 25,00 % | 9,84 |
| | | | UKUPAN IZNOS RAČUNA | | 196,57 |

Fig. 2 Excerpt from the invoice for charging at ZIR istok charging station

minutes of 9.84 HRK (as shown in Figure 2). We drove to Zagreb at lower speed, less acceleration, and we finally reached our destination with a state of charge of 25%.

Statistics for both trips are shown in the Table IV, generously shared by ELEN administrators. Interesting detail is that in the 2nd session, the charging duration was 65 minutes and 55 seconds (which would mean 5 minutes and 55 seconds or 5.92 min for penalty interval), but the application charged 69 minutes and 50 seconds (9.83 min for penalty interval).

TABLE III

CHARGING SESSIONS AT ZIR ZAPAD AND ZIR ISTOK

| Trip Zagreb – Šibenik | Trip Šibenik - Zagreb |
|---|---|
| S-2022/60550 | S-2022/60709 |
| Zir Zapad ultra DC | Zir Istok rapidna AC/DC |
| 28.6.2022. | 28.6.2022. |
| From 28.06.2022. 08:03:08 | From 28.06.2022. 17:18:06 |
| To 28.06.2022. 08:31:26 | To 28.06.2022. 18:24:02 |
| Vehicle 80% full at 28.06.2022. 08:21:28 | Vehicle 80% full at 28.06.2022. 18:23:06 |
| | Vehicle full at 28.06.2022. 18:24:02 |
| Connected from 28.06.2022. 08:02:40 | Connected from 28.06.2022. 17:14:19 |
| Connected to 28.06.2022. 08:31:53 | Connected to 28.06.2022. 18:24:09 |
| Charging with load to 28.06.2022. 08:30:38 | Charging with load to 28.06.2022. 18:24:02 |
| Charging with load duration 00:27:30 | Charging with load duration 01:05:55 |
| Time spent 00:28:18 | Time spent 01:05:55 |
| Energy consumption 57.96 kWh | Energy consumption 53.31 kWh |
| Max active power 161.26 kW | Max active power 49.03 kW |

Along with the table data for the two sessions, we also received a .csv data log of charging power and SoC, which is shown in the figure below for both sessions.

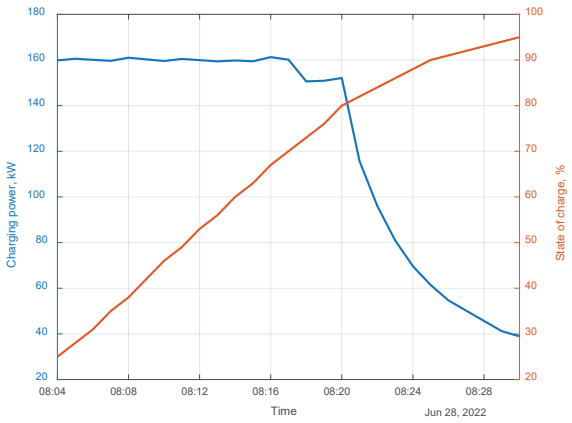


a) ZIR zapad ultra-fast DC charger

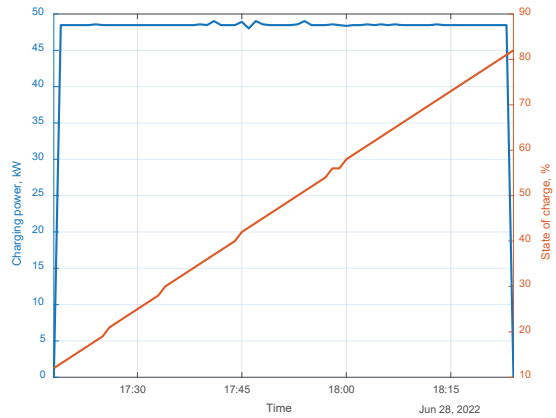


b) ZIR istok rapid AC/DC charger

Fig. 3. Charging profile obtained from data log

## C. ZAGREB – VOŠTANE

The primary goal of this trip was to reach the destination – a wind power plant (WPP) named VE Voštane in the south of Croatia, located 430 km from Zagreb, mostly on highway. The V2Load function of the vehicle was used to run the electrical equipment and a laptop while conducting field work in the wind power plant (Fig. 2).

Fig. 4. EV at the wind power plant site

Before starting the trip, a survey was conducted to find suitable charging stations at the destination location. There were no charging stations available on the WPP site, in the vicinity of the WPP, at the hotel we stayed overnight, and most disappointingly nor in the whole town of Sinj. The closest charging station was near the highway in Dugopolje. This was considered while planning the trip. The trip was started on Tuesday, 5 July 2022, with a fully charged EV.

The one-way distance via highway was 430 km, while the total trip length was 849 km, of which 75% was driven on highways. We charged the vehicle four times, for total of 1 h 44 min which resulted in 129.915 kWh of energy. The total price we paid was HRK 571.46 without tax. The overview of the trip is shown in Table IV.

TABLE IV

VOŠTANE TRIP OVERVIEW

| Feature | Trip 1 | Trip 2 | Trip 3 | Trip 4 | Trip 5 | Trip total |
|---|---|---|---|---|---|---|
| Mileage | 213 km highway | 227 km regional road | 108 km highway | 216 km highway | 81 km highway | 849 km |
| Cruise speed | 125 km/h | 80 km/h | 125 km/h | 125 km/h | 125 km/h | |
| Battery usage | 98% -> 29% | 99% -> 52% | 93% -> 61% | 75% -> 14% | 49% -> 22% | |

The first charging point we used was 213 km from Zagreb at the Mogorić station. At 125 km/h cruising speed, we arrived with 29% battery charge. At the charging station ELEN DC / 178 kW charger was immediately available and it took 35 minutes for the battery to gain 57.48 kWh. We left the station at 99% state of charge. Figure 5 shows the charging costs, 4.95 HRK/kWh with VAT.

We charged the vehicle the second time at the beginning of our return trip in Dugopolje. The vehicle state of charge was 52% after driving for 227 km on regional roads at 80 km/h and using the V2Load functionality. The Petrol DC / 160 kW charging station was available immediately and in 23 minutes we charged 33.05 kWh into the battery. This resulted in 93% state of charge and cost around 5 HRK/kWh (see Figure 6).


Hrvoje Pandžić, Bojan Franc, Stjepan Stipetić, Franko Pandžić, Matko Mesar, Marija Miletić, Sara Jovanović, Electric Vehicle Charging Infrastructure in Croatia – First-Hand Experiences and Recommendations for Future Development, Journal of Energy, vol. 71 Number 3 (2022), 16–23
https://doi.org/10.37798/2022713414

| stavka | količina | cijena kn | popust kn | stopa PDV | iznos kn |
|---|---|---|---|---|---|
| isporučena električna energija punionica 178,13 kW dan | 57,4840 kWh | 4,38 | | 13,00 % | 284,51 |
| | | | UKUPAN IZNOS RAČUNA | | 284,51 |

Fig. 5. Excerpt from the invoice for the 1st charging station (ELEN, Croatia)

| Tarifa | Stavka | Cijena | Količina | Stopa PDV | Iznos |
|---|---|---|---|---|---|
| Ultra brzo punjenje - trajna registracija | Naknada za potrošenu energiju | 4.4159 HRK/kWh | 33.0500 | 13.0% | 164.92 |
| ZA PLATITI HRK | | | | | 164.92 |

Fig. 6. Excerpt from the invoice for the 2nd charging station (Petrol, Croatia)

After 108 km of highway at 125 km/h we charged the vehicle for the third time at Nadin North station operated by ELEN. The DC charger rated at 50 kW was immediately available and we charged for 14 minutes from 61% to 75%. The energy charged was 12.78 kWh and it cost around 3.5 HRK/kWh (see Figure 7).

| stavka | količina | cijena kn | popust kn | stopa PDV | iznos kn |
|---|---|---|---|---|---|
| isporučena električna energija punionica 50 kW dan | 12,7830 kWh | 3,10 | | 13,00 % | 44,78 |
| | | | UKUPAN IZNOS RAČUNA | | 44,78 |

Fig. 7. Excerpt from the invoice for the 3rd charging station (ELEN, Croatia)

We charged the vehicle for the fourth time at Vukova Gorica station, after driving on highway for 216 km at 125 km/h. The ELEN DC / 50 kW charger was immediately available and in 32 minutes we charged 26.6 kWh into the battery. This took us from 14% to 49% state of charge and at night tariff cost around 2.9 HRK/kWh (see Figure 8).

| stavka | količina | cijena kn | popust kn | stopa PDV | iznos kn |
|---|---|---|---|---|---|
| isporučena električna energija punionica 50 kW noć | 26,5980 kWh | 2,57 | | 13,00 % | 77,25 |
| | | | UKUPAN IZNOS RAČUNA | | 77,25 |

Fig. 8. Excerpt from the invoice for the 4th charging station (ELEN, Croatia)

We charged the vehicle for the fifth and final time in Zagreb, at FER. The charging station was occupied for 3.5 hours and our vehicle was third in line. Charging lasted over 1.5 hours at 50kW rated charger. The vehicle was charged from 22% to 100%, taking in 60.06 kWh. As the charging station is operated by FER, the charging was done at no cost.

Generally, all the visited charging stations were operational, providing charge speeds as specified. DC chargers of speeds 50 kW (Fig. 14) and more were available at each charging points as specified. There were no waiting queues, no technical, software, nor any payment issues. Table V gives an overview of the charging data for this trip.


Fig. 9. Hyundai IONIQ 5 charging at Janjče ELEN charging station


Hrvoje Pandžić, Bojan Franc, Stjepan Stipetić, Franko Pandžić, Matko Mesar, Marija Miletić, Sara Jovanović, Electric Vehicle Charging Infrastructure in Croatia – First-Hand Experiences and Recommendations for Future Development, Journal of Energy, vol. 71 Number 3 (2022), 16–23
https://doi.org/10.37798/2022713414

TABLE V

VOŠTANE TRIP CHARGING DATA OVERVIEW

| Feature | Charge 1 | Charge 2 | Charge 3 | Charge 4 | Trip total |
|---|---|---|---|---|---|
| Charging station type | ELEN DC / 178 kW | Petrol DC / 160 kW | ELEN DC / 50 kW | ELEN DC / 50 kW | FER AC/DC 98 kW |
| Max power rated | 178 kW | 160 kW | 50 kW | 50 kW | 50 kW |
| Max power measured | 158 kW | 163 kW | 49 kW | 49 kW | not observed |
| Energy transferred | 57.48 kWh | 33.05 kWh | 12.78 kWh | 26.60 kWh | not observed |
| Charge time | 35 min | 23 min | 14 min | 32 min | not observed |
| Battery after charge | 99% | 93% | 75% | 49% | 100% |
| Price (without 13% tax) | 4.38 HRK / kWh | 4.42 HRK / kWh | 3.10 HRK / kWh | 2.57 HRK / kWh (night) | 571.46 HRK (w/o FER) |

On the way to the WPP Voštane, the first half of the trip was driven using the highway and at highway speed limits. Upon exiting the highway, the trip was continued with a fully charged EV. The second part of the trip was driven using regional roads at lower speeds. This change in driving speeds resulted in a dramatical increase of the EV's range, enabling us to reach the desired location with a higher-than-expected battery charge state. Although we started the trip with some range anxiety, due to knowing there are no charging points at our destination, after driving the regional roads and arriving at the target location with a more than 50% battery charge state, the range anxiety was completely gone.

On the way back, we charged the EV right away to (almost) full charge. The return trip was driven completely on the highway at speeds a bit under the speed limits (some experience was gathered on the first trip). Unfortunately, on the way back, in the direction from the Adriatic coast to Zagreb, there are no ultra-high-speed charging stations (so the tourists will leave the country after the vacation a bit slower than they arrived). All the charging stations visited were of max 50 kW DC, CCS2 / CHAdeMO. At the end of the trip, although battery charge levels dropped to 14%, there was no range anxiety as there are plenty of charging stations with free slots available. On the other hand, adding one and a half hour to a 5-hour trip took its toll and pushed us a step back to the old-fashioned internal combustion engine car.

### *D. Zagreb – Dubrovnik*

The trip started on Sunday, November 6 2022 around 8:50 in the morning with 94% of battery charge. This was the longest trip we took (around 650 km one-way) which turned out to be the most eventful and challenging as well. We tested the battery capacities on higher speeds in the first part of the trip so the first mandatory stop was Janjče Crodux gas station (Figure 10); 170 km from the starting point. The vehicle was charged using 50 kW CCS2 charger operated by ELEN from 16% to 44% battery capacity in 25 minutes (110 km of range). The whole experience was unpleasant as the designated app through which payment is done froze and crashed multiple times and emergency eject button had to be used to unplug the vehicle. Additional funds were reserved (HRK 400, which were subsequently refunded) for restarting the app and repeating the procedure of charging in an attempt to unplug the vehicle normally.

Fig. 10. Hyundai IONIQ 5 charging at Janjče ELEN charging station

The next stop was only 41 km away (gas station Zir) as the 160 kW ELEN supercharger was available. Everything went smoothly and in 20 minutes the battery was fully charged.

Dugopolje Petrol ABB was the next stop, 180 km away from Zir. The charging station was previously used in the Voštane trip and we expected good performance from it, which proved to be a mistake. Firstly, a new app had to be installed which was essentially the same as every other with a different logo. The charging would fail at the very last step where charger-vehicle communication couldn't be established. Both 50 kW CCS2 chargers behaved the same. For each charging attempt the app would reserve around HRK 450; in total over HRK 2200 for both chargers without actually providing any service. This created an additional problem as the funds were not promptly released. Furthermore, we were unable to resolve the issue through multiple attempts at contacting customer support. The only positive factor of this charging station was its close proximity to a shopping mall.

The next nearest charging station was a Tesla station which turned out to be unusable for other car manufacturers, as this service is not available in Croatia. Next, we tried HT Dugopolje charging station which either doesn't exist or was inaccessible, behind a closed fence. At this point, the battery range had decreased to less than 25 km, so extreme measures were taken to conserve power and avoid being stranded and further delayed with more complications. Another HT charging station in the nearby parking garage seemed to be the solution. Yet another app needed installing with a similar interface but slightly different functionalities. A card deposit of 50, 100, 200 or 500 HRK (only options) needed to be made to process eventual payment. Charging (50 kW CCS2) failed at the charger-vehicle communication again. This time customer support was available. Even though the information available online marked the station as functional, the support was aware of the issue. The customer support directed us to City Center One Split with assurance of a working charging station. Furthermore, the allocated funds through the app (HRK 200) were never refunded.

The City Center One Split charging station wasn't easy to find because of insufficient instructions on the parking lot. It was a 22 kW output but no charging cable was provided. We used our own cable with which we were able to utilize only 11 kW of power. The usage instructions were also confusing as it stated requirement of another app being installed but turned out to be free of charge. The charging time was 1h to gain 11 kWh or 40 km of range (15 to 55 km) just to be able to make it to a higher output charger at the highway.

The next station was a much needed 50 kW ELEN charger in Dračevac, Split, pictured below. A 30 min charging process was enough for additional 167 km of range (19% – 55% of battery charge). The charger was located in the middle of nowhere surrounded by what seemed to be a make-shift waste disposal but was easy to find using online instructions and was functional. As the destination was still 250 km away, another stop was deemed necessary to be certain and avoid any further unpleasantries.

Fig. 11. Hyundai IONIQ 5 charging at Dračevac ELEN charging station

The last stop before the destination was Rašćane Gornje gas station back on the highway where another ELEN 50 kW CCS2 charger was located. The charger was hard to find on the large parking lot at night as it wasn't marked or illuminated in any way. The final charge of the trip took 77 mins in total (26 – 81 % in 53 mins, 81 – 89 % in 9 mins and 89 – 100 % in 15 mins). Upon arriving to the destination in Cavtat, the battery charge was 65 % with an estimated range of 203 km. The time of arrival was around 22:30 h. In other words, a trip of 650 km (with detours and charging) took almost 14 hours to complete. On a scale of 0 to 10, we would rate the experience as 1 just for the sake of making it to the destination.

Valuable insight was gained during this trip:

- Charging stations in Croatia that are located off the highway and outside of peak tourist season are often poorly maintained or not maintained at all and are to be avoided if possible.
- Charging stations along the highway seem to be functional and responsive and are recommended.
- Customer support for some chargers (Petrol) is unavailable either outside tourist season or on weekends.
- Power consumption must be frugal during long trips with electric vehicles, even more than expected.
- ELEN charging stations proved the most trustworthy, but the reason might be their placement on the highway, while the Petrol and HT stations were located next to shopping centers.
- Have trip companions to kill time and have more resources.

## IV. Conclusion

This paper provided first-hand long-trip experiences with a Hyundai Ioniq 5 with a large-capacity battery in Croatia during 2022. These trips ranged from 340 km in each direction, i.e. Zagreb-Šibenik, to over 600 km in each direction when traveling from Zagreb to Dubrovnik. The trips predominantly used fast highways. We did not experience issues with the vehicle itself, but we did experience issues with the charging infrastructure. Our observations are as follows:

- Croatian highways are equipped with enough charging stations. However, more than several charging sessions required calling the customers' service to start the charging process. Such user experience is simply not good enough in times when the sales of electric vehicles is about to pick up and become predominant. Moreover, fast charging stations are available only in one direction of the highway which makes the trips from the coast toward Zagreb slower.
- More serious issues are related to poor directions for reaching charging stations located outside the highways (both in Croatia and Austria) and communication errors making the charging impossible. As opposed to gas stations, which pretty much always have enough gas to fuel any vehicle, which are predominantly open non-stop and which have a person operating the station, the fact that there is no live person to help with the EV charging process makes drivers uncomfortable and always in need of plan B.
- Charging an electric vehicle at different locations and countries calls for installation and getting used to multiple apps, which wastes a lot of the drivers' time.
- We did not experience waiting times for a charging station to free up, however, that could be a serious issue during the tourist season.
- Charging times are still long, even with fast charging stations operating at 50 kW, which is the most common type of stations. For a high-capacity battery this still requires over one hour to charge, which is simply a lot, especially as there is not much to do while the vehicle is charging. An idea might be to couple fast charging stations with entertainment centers, e.g. shopping malls, restaurants, children fun centers, etc., to make long waiting times easier to handle.
- Electric vehicle, at least with the current charging infrastructure, calls for different driving style. Namely, if a 50 kW fast charging station is the fastest charging option, the most time-efficient driving speed is just above 100 km/h. Faster driving significantly reduces the range, and since the battery takes a lot of time to charge, the overall traveling time is increased. This is a major difference as compared to the petrol or diesel cars.
- Ultra-high-speed charging stations (180 kW and above) are a great solution for electric vehicle drivers on highway, as the vehicle is charged within 15-20 minutes, which is bearable for most drivers. However, such stations are scarce both in Croatia and Austria. In Croatia, currently there is only a single ultra-high-speed charging station on the highway from Zagreb to the south, and zero in the opposite direction. Similarly, it takes some severe detours in Austria to reach ultra-high-speed charging stations. The situation is somewhat better in Slovenia, which has few ultra-high-speed charging stations at gas pumps located on highways.

To conclude, the charging infrastructure requires better planning and the current experience is still not satisfactory for a regular driver. Focus should be put on high-speed charging stations that would make the charging experience very similar to the one at the gas stations. However, the development of ultra-high-speed charging stations is not economic to the charging point operators as the connection costs and peak (monthly) power cost are too expensive to be paid off through an infrequent use of the charging points.


Hrvoje Pandžić, Bojan Franc, Stjepan Stipetić, Franko Pandžić, Matko Mesar, Marija Miletić, Sara Jovanović, Electric Vehicle Charging Infrastructure in Croatia – First-Hand Experiences and Recommendations for Future Development, Journal of Energy, vol. 71 Number 3 (2022), 16–23
https://doi.org/10.37798/2022713414

## References


[1] V. Bobanac, H. Bašić, and H. Pandžić, "Determining Lithium-ion Battery One-way Energy Efficiencies: Influence of C-rate and Coulombic Losses", in *IEEE EUROCON 2021 - 19th International Conference on Smart Technologies*, Jul. 2021, pp. 385–389. doi: 10.1109/EUROCON52738.2021.9535542.

[2] L. Punda, T. Capuder, H. Pandžić, and M. Delimar, "Integration of renewable energy sources in southeast Europe: A review of incentive mechanisms and feasibility of investments", *Renew. Sustain. Energy Rev.*, vol. 71, pp. 77–88, May 2017, doi: 10.1016/j.rser.2017.01.008.

[3] I. Vassileva and J. Campillo, "Adoption barriers for electric vehicles: Experiences from early adopters in Sweden", *Energy*, vol. 120, pp. 632–641, Feb. 2017, doi: 10.1016/j.energy.2016.11.119.

[4] M. Gržanić, A. Hrga, and T. Capuder, "Profitable Investment in PV and BES Integrated with EV Charging Stations in Croatia - Myth or Reality?", in *2022 7th International Conference on Smart and Sustainable Technologies (SpliTech)*, Jul. 2022, pp. 1–6. doi: 10.23919/SpliTech55088.2022.9854341.

[5] "EU ban on sale of new petrol and diesel cars from 2035 explained | News | European Parliament", Nov. 03, 2022. https://www.europarl.europa.eu/news/en/headlines/economy/20221019STO44572/eu-ban-on-sale-of-new-petrol-and-diesel-cars-from-2035-explained (accessed Apr. 13, 2023).

[6] S. Hardman *et al.*, "A review of consumer preferences of and interactions with electric vehicle charging infrastructure", *Transp. Res. Part Transp. Environ.*, vol. 62, pp. 508–523, Jul. 2018, doi: 10.1016/j.trd.2018.04.002.

[7] *Directive (EU) 2018/844 of the European Parliament and of the Council of 30 May 2018 amending Directive 2010/31/EU on the energy performance of buildings and Directive 2012/27/EU on energy efficiency (Text with EEA relevance)*, vol. 156. 2018. Accessed: Apr. 13, 2023. [Online]. Available: http://data.europa.eu/eli/dir/2018/844/oj/eng

[8] *Directive (EU) 2018/2001 of the European Parliament and of the Council of 11 December 2018 on the promotion of the use of energy from renewable sources (recast) (Text with EEA relevance.)*, vol. 328. 2018. Accessed: Apr. 13, 2023. [Online]. Available: http://data.europa.eu/eli/dir/2018/2001/oj/eng

[9] N. Čović, F. Braeuer, R. McKenna, and H. Pandžić, "Optimal PV and Battery Investment of Market-Participating Industry Facilities", *IEEE Trans. Power Syst.*, vol. 36, no. 4, pp. 3441–3452, Jul. 2021, doi: 10.1109/TPWRS.2020.3047260.

[10] E. Sunnerstedt, M. Xylia, and A. Sjögren, "The City of Stockholm experiences with charging infrastructure for EVs", in *32nd International Electric Vehicle Symposium (EVS32)*, Lyon, Mar. 2019.

[11] M. Emanović, M. Jakara, and D. Barić, "Challenges and Opportunities for Future BEVs Adoption in Croatia", *Sustainability*, vol. 14, no. 13, Art. no. 13, Jan. 2022, doi: 10.3390/su14138080.

[12] M. Mutavdžija, M. Kovačić, and K. Buntak, "Assessment of Selected Factors Influencing the Purchase of Electric Vehicles—A Case Study of the Republic of Croatia", *Energies*, vol. 15, no. 16, Art. no. 16, Jan. 2022, doi: 10.3390/en15165987.

[13] I. Pavić, N. Holjevac, M. Zidar, I. Kuzle, and A. Nešković, "Transportation and power system interdependency for urban fast charging and battery swapping stations in Croatia", in *2017 40th International Convention on Information and Communication Technology, Electronics and Microelectronics (MIPRO)*, May 2017, pp. 1465–1470. doi: 10.23919/MIPRO.2017.7973652.

[14] T. Capuder, D. Miloš Sprčić, D. Zoričić, and H. Pandžić, "Review of challenges and assessment of electric vehicles integration policy goals: Integrated risk analysis approach", *Int. J. Electr. Power Energy Syst.*, vol. 119, p. 105894, Jul. 2020, doi: 10.1016/j.ijepes.2020.105894.

[15] J. J. Bakker, "Contesting range anxiety : the role of electric vehicle charging infrastructure in the transportation transition", Master, Eindhoven University of Technology, Eindhoven, 2011.

[16] P. Chakraborty *et al.*, "Addressing the range anxiety of battery electric vehicles with charging en route", *Sci. Rep.*, vol. 12, no. 1, Art. no. 1, Apr. 2022, doi: 10.1038/s41598-022-08942-2.

[17] H. Pandžić *et al.*, "Ioniq 5 Trips", 2022. https://www.google.com/maps/d/edit?mid=1Kez_o-rZmHD4pY1DqRJqP2bnQ6w9MQo&usp=sharing (accessed Apr. 13, 2022).

Journal of Energy

VOLUME 71 Number 3 | 2022

journal homepage: http://journalofenergy.com/

# TARGET – Development of Submersible ROV System for BMN Inspection

Josip Arland, Krunoslav Markulin, Nikola Pavlović

***Summary* — Most PWRs have penetrations in the RPV lower heads for in-core nuclear instrumentation. These penetrations generally are made of nickel-based Inconel Alloy 600. Weld materials are typically Alloy 82/182. Operating conditions of PWR plants are causing nickel-based alloys cracking through a process called primary water stress corrosion cracking (PWSCC). In 2003, the licensee for the South Texas Project Unit 1 (STP-1) identified apparent boron deposits on the lower RPV head near two bottom mounted nozzles (BMNs). The NRC issued Bulletin 2003-02 to obtain information on licensee inspection activities and inspection plans for the RPV lower head. EPRI issued MRP-206 report that provides inspection and evaluation guidelines for BMNs for PWR plants, including guidelines for periodic bare metal visual examination for evidence of primary coolant leakage, or periodic non-visual nondestructive examinations for indications of service-induced cracking. The non-visual inspections (ultrasonic testing examination) may detect service-induced degradation before through-wall cracking, leakage, circumferential cracking below the bottom of the J-groove weld, release of loose parts, or incipient boric acid wastage of the low-alloy steel reactor vessel lower head material occurs. Therefore, periodic examinations will adequately manage potential for cracking by PWSCC and preserve structural integrity. INETEC developed TARGET system for BMNs inspection, consisted of submersible ROV and specially designed probe, composed of several UT probes. UT system and technique to detect, length and depth size the service-induced degradation in the BMN volume material is developed. The EPRI NDE Center performed a technical review and validated INETEC's ultrasonic examination technique for BMNs. Aforementioned validation was done according to requirements defined by: 1) MRP-206, 2) MRP-411.**

***Keywords* — Submersible ROV, BMN Inspection, nondestrucitve examination, ultrasonic testing examination, ultrasonic examination technique**

## I. Introduction

Most pressurized water reactor (PWR) type of nuclear power plants have penetrations in the reactor pressure vessel (RPV) lower heads for in-core nuclear instrumentation. The RPV bottom mounted nozzles (BMN) in PWR are fabricated from nickel-chromium-iron Alloy 600 [1]. J-groove welds connect BMNs to the lower head of the RPV and is usually made from Alloy 82 and/or Alloy 182 [1]. These components are susceptible to age-related degradation due to primary water stress corrosion cracking (PWSCC) [1].

In the spring of 2003, the licensee for the South Texas Project Unit 1 (STP-1) identified apparent boron deposits on the lower RPV head near two BMNs [2]. The NRC issued Bulletin 2003-02 to obtain information on licensee inspection activities and inspection plans for the RPV lower head [3]. In October, 2013, during a scheduled visual examination of the BMNs at Palo Verde Nuclear Generating Station Unit 3, white residue around the BMNs were identified [1]. Nondestructive examinations confirmed that axial cracking at the nozzle weld was responsible for the leakage [1]. Periodic visual examinations of the BMNs are specified in ASME Code Case N-722-1 [4]. The examination is performed from the exterior of the reactor coolant system for evidence of leakage, such as boron or corrosion product deposits [4]. In alternative to Code Case N-722-1, Electric Power Research Institute (EPRI) issued "Materials Reliability Program: Inspection and Evaluation Guidelines for Reactor Vessel Bottom-Mounted Nozzles in U.S. PWR Plants (MRP-206). This report provides guidelines not only for visual examination, but also for periodic non-visual nondestructive examinations for indications of service-induced cracking. The non-visual inspections such as ultrasonic testing examination, may detect service-induced degradation before through-wall cracking, leakage, circumferential cracking below the bottom of the J-groove weld, release of loose parts, or incipient boric acid wastage of the low-alloy steel reactor vessel lower head material occurs [2]. Periodic examinations will adequately manage potential for cracking by PWSCC and preserve structural integrity. Therefore, INETEC developed new system for inspection of Westinghouse PWR 2-loop. 3-loop and 4-loop type of BMNs.

## II. Bottom Mounted Nozzle

The attachment of the BMN (Figure 1) to the bottom head consisted of either Alloy 182 or Alloy 82 weld metal in a prepared J-groove, which was machined into the inside surface of the vessel adjacent to each previously drilled penetration hole. The design of the J-groove was essentially the same for all plants. The BMNs examination volume (Figure 2) is 25.4 mm below the lowest point of the root of the J-groove weld to the highest point at the toe of the J-groove weld. A-B-C-D volume is extent of volumetric examination for the tube (base metal) [5].

(Corresponding author: Josip Arland)

Josip Arland, Krunoslav Markulin and Nikola Pavlović are with the INETEC – Institute for Nuclear Technology Lučko, Croatia (Josip.arland@inetec.hr, Krunoslav.markulin@inetec.hr, Nikola.pavlovic@inetec.hr)



Josip Arland, Krunoslav Markulin, Nikola Pavlović, TARGET – Development of Submersible ROV System for BMN Inspection, Journal of Energy, vol. 71 Number 3 (2022), 24–28
https://doi.org/10.37798/2022713416

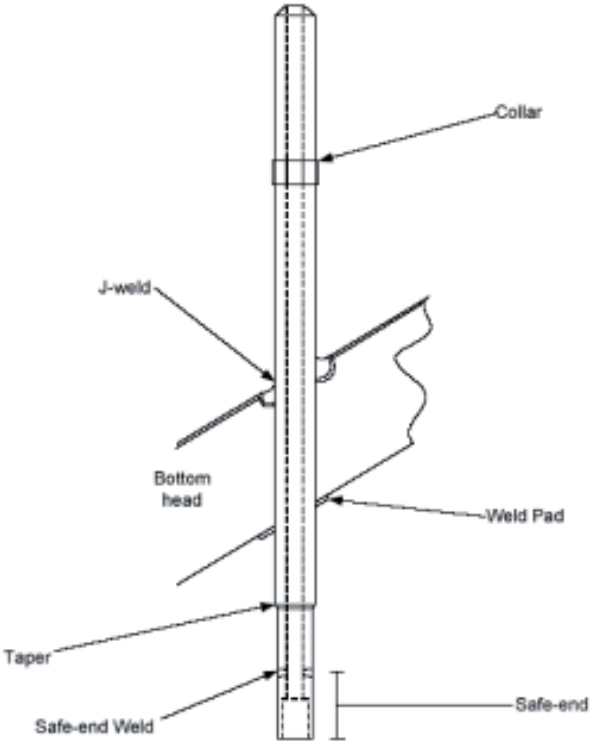


Fig. 1. Westinghouse-designed BMN [5]

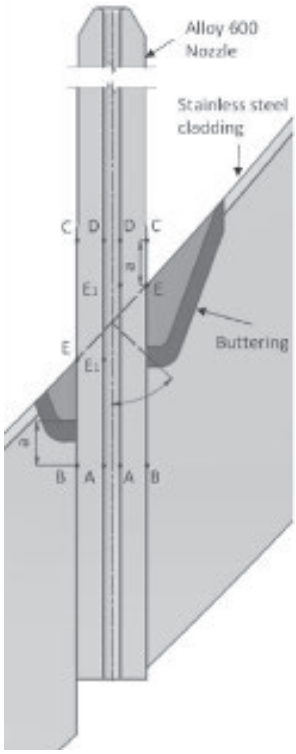


Fig. 2. BMN examination volume [5]

## III. TARGET Inspection System

The TARGET inspection system is designed to perform the complete ultrasonic examination of BMNs in reactor pressure vessel, which provides probe movement, and with control system that controls tool and generates position pulses. Schematic description of the inspection system is shown below (Figure 3).

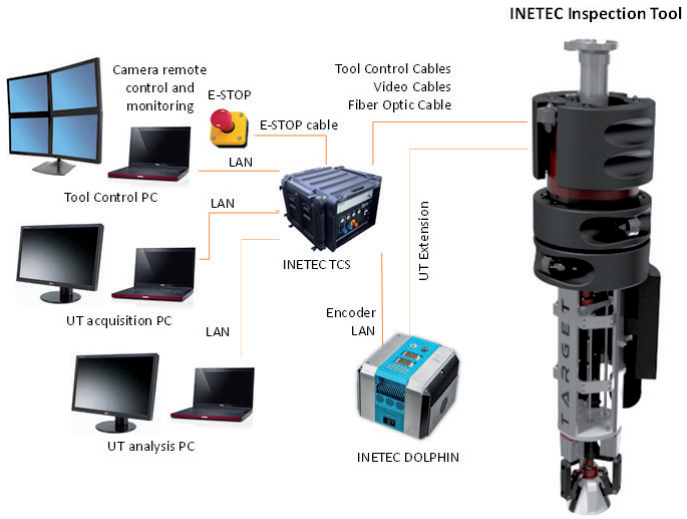


Fig. 3. Schematic description of the TARGET inspection system [5]

### A. TARGET

TARGET is remotely operated vehicle (ROV) that is able to work underwater. Once underwater, there is no need for any type of crane to support the ROV. It has propulsion system using thrusters to navigate itself. Bell like design of bottom of the ROV facilitates navigation to the top of BMN. Centering and fixating of the ROV is done with gripper that is pneumatically actuated (Item 3, Figure 4). There are two motor driven axes for the probe translation (Item 1, Figure 4) and rotation (Item 2, Figure 4). Both axes are have predetermined positions where each axis can be calibrated. To avoid any type of accident during scanning, multiple safety precautions are introduced. Both mechanical and software limits are set to prevent probe from breaking.

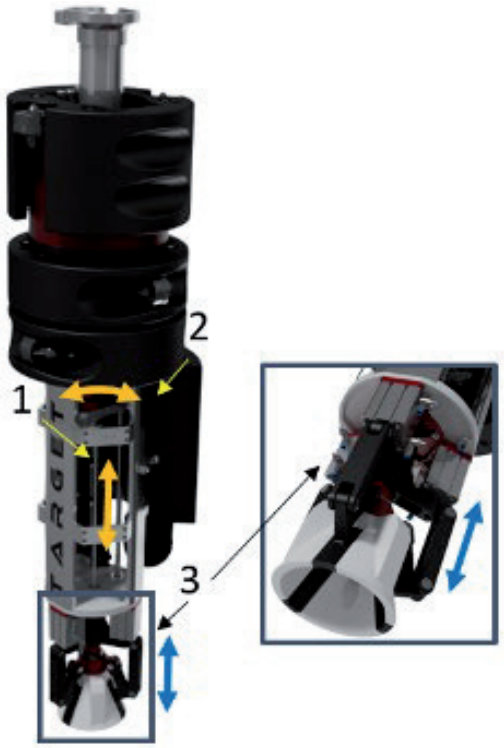


Fig. 4. TARGET – Degrees of freedom driven by motors and pneumatic cylinders
1) Probe translation; 2) Probe rotation; 3) Gripper extension/retraction.


Josip Arland, Krunoslav Markulin, Nikola Pavlović, TARGET – Development of Submersible ROV System for BMN Inspection, Journal of Energy, vol. 71 Number 3 (2022), 24–28
https://doi.org/10.37798/2022713416

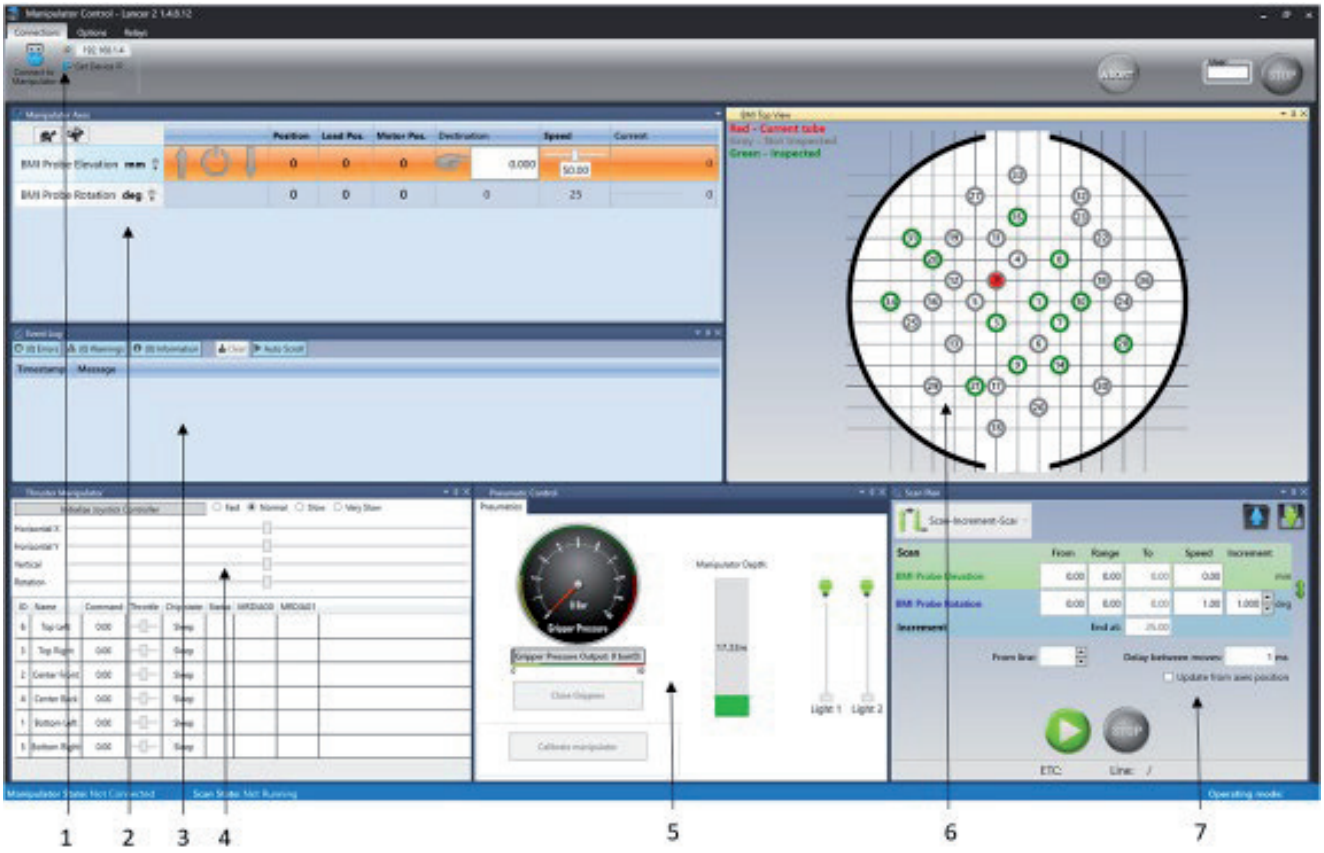


Fig. 5. Manipulator control software layout
1) Ribbon menus; 2) Axes controls; 3) Event log window; 4) Thruster controls; 5) Pneumatics panel; 6) Visualization window; 7) Scan plan control.

Neutral buoyancy of the ROV enables easy navigation through the water. On the ROV itself, two cameras are placed to help operator navigate the ROV on chosen BMN. Additional camera on side of the ROV is placed for the surveillance.

TARGET is operated through manipulator control software (Figure 5). Manipulator Control software supports two modes of operation – the standard mode and the admin mode. The standard mode is designed so the ROV can always be driven safely, without the possibility of accidentally causing it to behave incorrectly. The admin mode allows the user full control over the ROV and can only be accessed with an administrator password. Additionally, for the ease of navigation and driving through the water one can initialize joystick controller.

## *B. UT DATA COLLECTION*

UT data is obtained via INETEC's Dolphin 128/128 PR (Figure 6). It is a phased-array ultrasonic instrument with support for all common ultrasonic inspection techniques. It comes in an industrial grade housing and easily fit into a multitude of inspection system scenarios.

Fig. 6. Dolphin 128/128 PR UT instrument [5]

INETEC designed new type of probe for the BMN inspection, called "PRO ULTRA TARGET". It has multiple variants depending on the ID/OD diameters for different BMN penetrations. Each probe is composed of three pairs of time of flight diffraction (TOFD) transducers (one axial and two circumferential) and one 0° longitudinal wave probe.

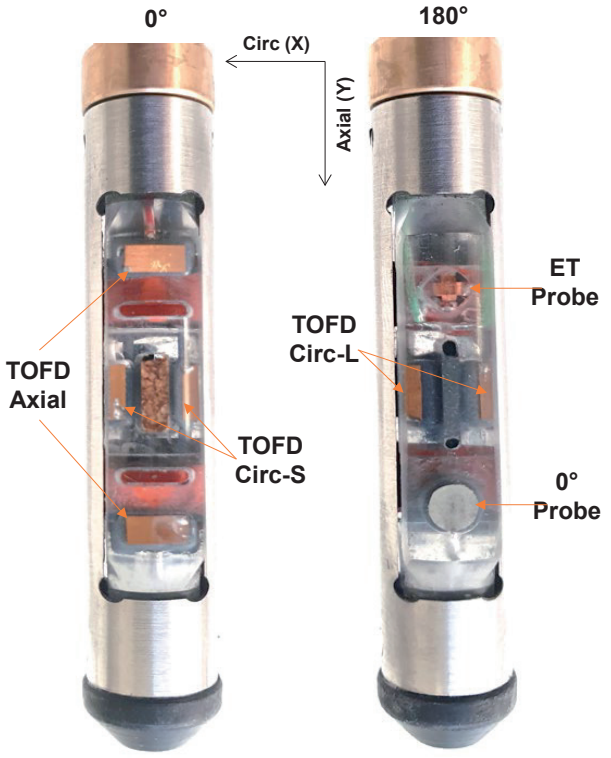


Fig. 7. "PRO ULTRA TARGET" probe [5]


Josip Arland, Krunoslav Markulin, Nikola Pavlović, TARGET – Development of Submersible ROV System for BMN Inspection, Journal of Energy, vol. 71 Number 3 (2022), 24–28
https://doi.org/10.37798/2022713416

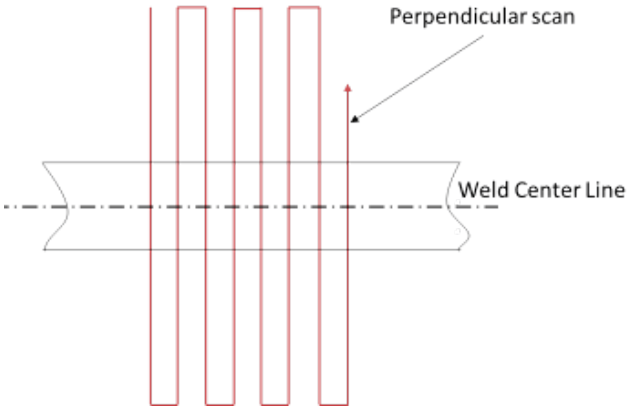

Figure 8. Scan pattern [5]

Probe is translated and rotated using two motor axes. Scan pattern is shown in the Figure 8. Inside the ROV, secondary calibration of the probe could be performed. With this approach it reduces unnecessary movement and loss of precious time during inspection. Evaluation of the data is performed using INETEC's SignyOne software. Standard C-scan, B-scan and A-scan combination is used for data evaluation.

## IV. Inspection Methodology

INETEC's approach to ISI of BMNs is result of experience on similar inspections and improvements as a result of gathered experience and lesson learned.

For the BMN inspection remotely controlled TARGET is used. Operator's workstation is situated outside of the reactor building and radiologically controlled area, thus minimizing radiological exposure and reducing necessary space reservation inside the containment.

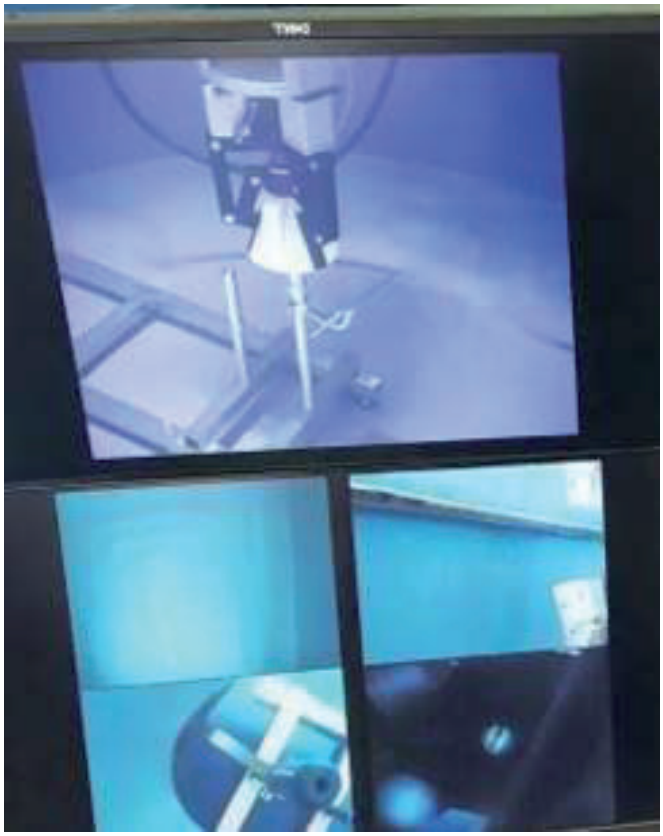
Figure 9. Positioning TARGET on top of BMN

Communication from inside to the outside of the containment is done using fiber optics cables through available penetration. TARGET is deployed in water with remote docking tool. It is pneumatically actuated assembly of rods that are used to transfer different INETEC manipulators from their respective stand to the water. After the TARGET is submerged into the reactor vessel water, remote docking tool is disconnected and the ROV is driven down to BMNs by using thruster propulsion system. TARGET functionality, installation, inspection and probe movements are monitored with several cameras installed on TARGET (Figure 9) for precise adjustments above BMN and fine positioning. Once the TARGET is positioned on top of BMN, it can be gripped using pneumatic cylinders. All axes can be calibrated by using reference locations defined by limit switches. Furthermore, for probe calibration secondary calibration block is available. Defining scan plan according to applicable standards operator can start the examination. Probe movement is shown in Figure 8. Once the scan is over, probe returns to home position in which it is enabled to detach the ROV from BMN.

## V. Qualification

INETEC developed a UT technique and probe to perform demonstration for examination of bottom mounted nozzles. EPRI BMN Westinghouse 2, 3 and 4 loop flawed mockups were provided to INETEC. Six BMN mockups were examined: two Westinghouse two loop mockups; two Westinghouse three loop mockups, and two Westinghouse four loop mockups. All acquired data was evaluated by INETEC and provided to EPRI for independent review.

Each mockup has multiple flaws that are manufactory processed. Flaw manufacturing processes may include cold isostatic processing (CIP), hot isostatic processing (HIP), laboratory-grown stress corrosion cracks (SCC), weld contamination flaws, and/or a combination of these processes. The mockups contain the axial/radial and circumferential/radial flaws in the tube located above, below, and/or over the attachment weld area.

In order to prove theoretical presumptions and newly designed probe, INETEC evaluated mockups to document basic flaw detection, location capabilities, characterization and length and depth sizing on representative mockups. It was performed in a non-blind fashion. INETEC personnel collected and analysed data (Figure 10) in accordance to INETEC procedure. The UT results including raw data were provided to EPRI to perform a technical review and for validation of technical justification versus raw data.

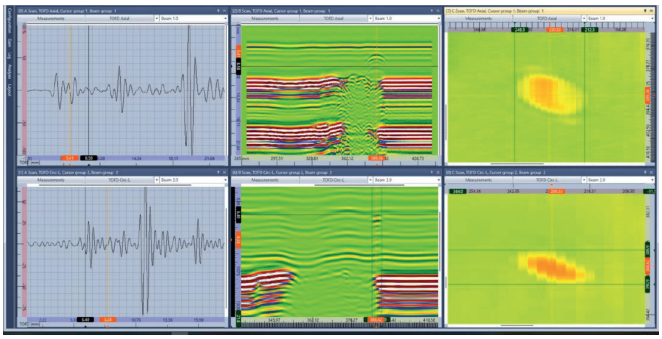
Figure 10. OD flaw on a mockup [5]


Josip Arland, Krunoslav Markulin, Nikola Pavlović, TARGET – Development of Submersible ROV System for BMN Inspection, Journal of Energy, vol. 71 Number 3 (2022), 24–28
https://doi.org/10.37798/2022713416

## VI. CONCLUSION

INETEC developed new remotely controlled TARGET system for BMN inspection. Once submerged, it becomes independent from polar crane or refuelling bridge, thus reducing unnecessary time loss for maintenance operations. Its ease of navigating and operating helps it to move quickly on designated BMN. For UT data collection, INETEC uses its own Dolphin, phased-array ultrasonic instrument with support for all common ultrasonic inspection techniques. Furthermore, INETEC developed probe "PRO ULTRA TARGET" with multiple variants for different Westinghouse type of BMNs. Probe is composed of three pairs of time of flight diffraction (TOFD) transducers (one axial and two circumferential) and one 0° longitudinal wave probe. Demonstration of examination of bottom mounted nozzles was performed and UT technique was developed on previously delivered flawed mockups given by EPRI. In order to prove theoretical presumptions and newly designed probe, INETEC evaluated mockups to document basic flaw detection, location capabilities, characterization and length and depth sizing on representative mockups. All acquired data was evaluated by INETEC and provided to EPRI for independent review. Review showed that INETEC demonstrated capabilities of the system that satisfied demands for proper flaw detection and characterization.

## REFERENCES


[1] Materials Reliability Program: PWR Bottom Mounted Nozzle (BMN) Non-destructive Examination Technical Basis (MRP-411). EPRI, Palo Alto, CA: 2020. 3002007948.

[2] Materials Reliability Program: Inspection and Evaluation Guidelines for Reactor Vessel Bottom-Mounted Nozzles in U.S. PWR Plants (MRP-206). EPRI, Palo Alto, CA: 2009. 1016594.

[3] NRC Bulletin 2003-02: Leakage from Reactor Pressure Vessel Lower Head Penetrations and Reactor Coolant Pressure Boundary Integrity. United States Nuclear Regulatory Commission, Washington, DC: 2003.

[4] ASME Code Case N-722-1, "Additioinal Examinations for PWR Pressure Retaining Welds in Class 1 Components Fabricated with Alloy 600/82/182 Materials, Section XI, Division 1" ASME, January 26, 2009.

[5] Technical Justification for Ultrasonic Examination of Reactor Vessel Bottom Mounted Nozzle (BMN) Head Penetrations in Westinghouse 2, 3 and 4 Loop Plants. INETEC, Zagreb, 2021.

Journal of Energy

VOLUME 71 Number 3 | 2022

journal homepage: http://journalofenergy.com/

# Bus Split Contingency Analysis Implementation in the NetVision DAM EMS

Frano Tomašević, Vlatko Debeljuh, Renata Rubeša, Ana Jukić, Krešimir Mesić, Marko Kodrin

***Summary* — Implementation of the bus coupler outage scenarios, commonly known as bus splitting, in the NetVision DAM energy management system (EMS) contingency analysis is presented in this paper. In order to identify the bus coupler branches in the network model, the existing topology processor was upgraded. The description of the topological algorithm for detection of the bus couplers is given. Based on the topology analysis results, calculation subnodes are created. Calculation model was modified in order to include the bus couplers and the subnodes as the new calculation objects. These modifications are fundamental for the introduction of the bus coupler outages in the contingency analysis. Implications of the bus coupler outages on the load flow mathematical model are discussed. Implemented NetVision DAM solution for the analysis of such outage scenarios is presented.**

***Keywords* — power system, contingency analysis N-1, bus coupler outage, bus splitting**

## I. Introduction

Reliable security assessment is one of the most important tasks in the power system control and planning. Such security assessments are most often based on the results of the contingency analysis calculations for the power system stationary state. The main objective is the identification of outages which could cause the violation of the power system operational constraints. Most often the N-1 criterion, in which only the single element outages are analysed, is used. However, in certain cases multiple outages are also taken into account (N-k criterion), especially the case of simultaneous outage of two power system objects (N-2 criterion).

Contingency analysis is based on the sequential load flow calculations for the pre-defined outage scenarios. Generally, such scenarios include outages of the overhead transmission lines, high-voltage power cables, transformers, synchronous generators and compensation devices. On the other hand, outages of elements that are not explicitly and unambiguously represented in the commonly used bus-branch power system calculation model, such as the bus coupler circuit breakers, are analysed to a much lesser extent.

The inclusion of the bus coupler outages, also commonly known as the bus splitting events, in the contingency analysis is becoming more and more important, due to the increasingly frequent circuit breakers misoperations [1], [2] or malicious cyberattacks [3] – [7]. The bus coupler circuit breakers states determine the topological interpretation of the switchgear, and therefore the overall mathematical (calculation) model of the power system [8]. The node-breaker representation includes detailed modelling of all the substation components. The bus couplers are usually modelled as (near) zero impedance lines [9] - [11], and their implementation in the contingency analysis is similar to the line outage calculations. However, the node-breaker model typically involves sparse matrices of much larger dimensions due to the significant increase in the number of the nodes [12]. The bus-branch model, on the other hand, lacks the detailed substation information, and cannot directly include the bus split event in the contingency analysis [12]. However, because of its simplicity and efficiency, it is still a most commonly used EMS model.

Additionally, the bus-branch model can be modified in order to implement the bus coupler circuit breaker switching actions. The bus coupler outage scenario has a specific impact on the mathematical interpretation of the transmission grid topology state (i.e. bus admittance matrix), considering it requires the change in the number of the bus-breaker model calculation nodes. Therefore, the analysis of such scenarios requires the application of different mathematical models, in comparison with the conventional outages, i.e. outages of elements such as the transmission lines or the transformers.

Modifications of the topological processor are required in order to enable the detection of the active bus couplers, i.e. active circuit breakers which represent the connection between the two active busbars. If such bus coupler is detected within the station voltage level, new subnodes are created and assigned to the corresponding calculation node. These subnodes represent only the potential calculation nodes which, in the case of the bus coupler outage, become real, and are used as such in the contingency analysis calculations.

(Corresponding author:



Frano Tomašević, Vlatko Debeljuh, Renata Rubeša, Ana Jukić, Krešimir Mesić, Marko Kodrin, Bus Split Contingency Analysis Implementation in the NetVision DAM EMS, Journal of Energy, vol. 71 Number 3 (2022), 29–33
https://doi.org/10.37798/2022713422

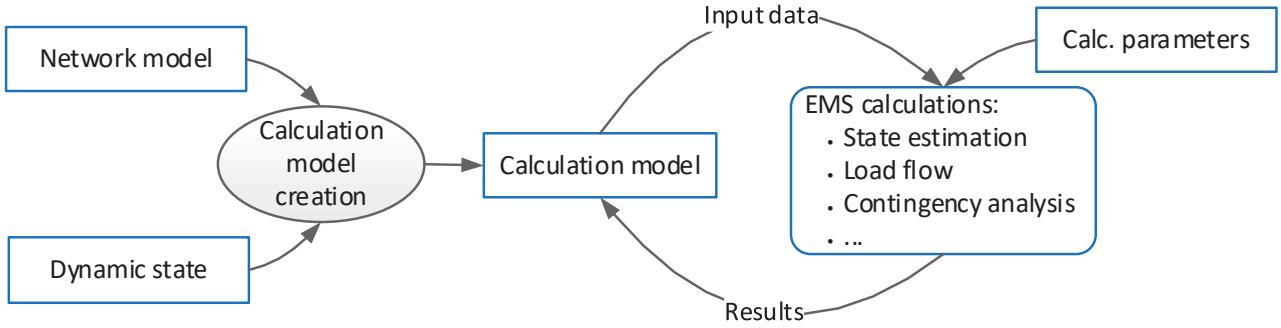


Fig. 1. Basic architecture of the NetVision DAM EMS

## II. Power system modelling

All calculations in the NetVision DAM EMS are based on the so-called calculation model, which basically represents the mathematical bus-branch interpretation of a single power system stationary state [13], [14]. The fundamental architecture of such model is very simple, as it consists solely of calculation nodes and branches. Calculation nodes represent mathematical equivalents of the parts of the network which have the same electrical potential. Typically, a node represents a substation of a certain nominal voltage which includes a group of interconnected sections and fields with the substation objects such as busbars, breakers, disconnectors, etc. Nodes are interconnected by branches. Branches represent power system objects such as the transmission lines, the transformers and the high voltage power cables. Other power system elements, such as the shunt compensation devices or the fixed impedance loads, are also modelled as branches, incident with a single node and the ground.

NetVision DAM calculation model is created using the two data sources: the network model, and the dynamic data (Fig. 1). The network model is a detailed, hierarchical and topologically organized representation of all existing power system elements. In comparison with the calculation model, it contains significantly larger data set. As such, it is generally unsuitable for the direct use in the calculations. Therefore, it represents a main source of fixed data (parameters) required for the creation of the calculation model objects. The dynamic state includes all the real process data, measurements and signals collected from the transmission grid using the SCADA system. The working topology of the analysed grid is created using the topology processor, based on the collected breaker and the disconnector states. Topology is created using the depth first search (DFS) algorithm, firstly on the substation level, and then the network level. After the topology is created, the SCADA measurements are preprocessed and joined with the corresponding calculation model objects. Finally, they are used for the creation of the input data vectors for the EMS calculations. Therefore, the calculation model is completely defined by the three data groups: the topological state, the fixed parameters of the power system elements, and the input data measurements.

## III. Bus coupler identification

The result of the topological analysis is a graph model, which is a mathematical model consisting of nodes and branches. Each branch connects two nodes, and can be classified as oriented or non-oriented. The graph model and the standard graph algorithms have been upgraded for the needs of the transmission grid modelling and analysis. The basis for all the graph analysis in the NetVision DAM is the DFS algorithm, which, in its fundamental form, detects the connected graph parts, that is the connectivity components [16], [17]. The connectivity components are the sets of the connected graph nodes, which are used to create the dynamic model nodes. Modified algorithm detects bridges, separation nodes, blocks containing loops, connecting paths, etc.

From each substation voltage level, a corresponding graph is formed, in which the circuit breakers and the disconnectors represent branches connecting the graph nodes (external nodes, grounding, buses, etc.). Unlike the station topology, the network topology is defined by the graph in which the branches represent the transmission lines, high-voltage cables and transformers incident with the external station nodes. Other objects, such as the generators, loads and shunt compensators, are also connected to the external station nodes.

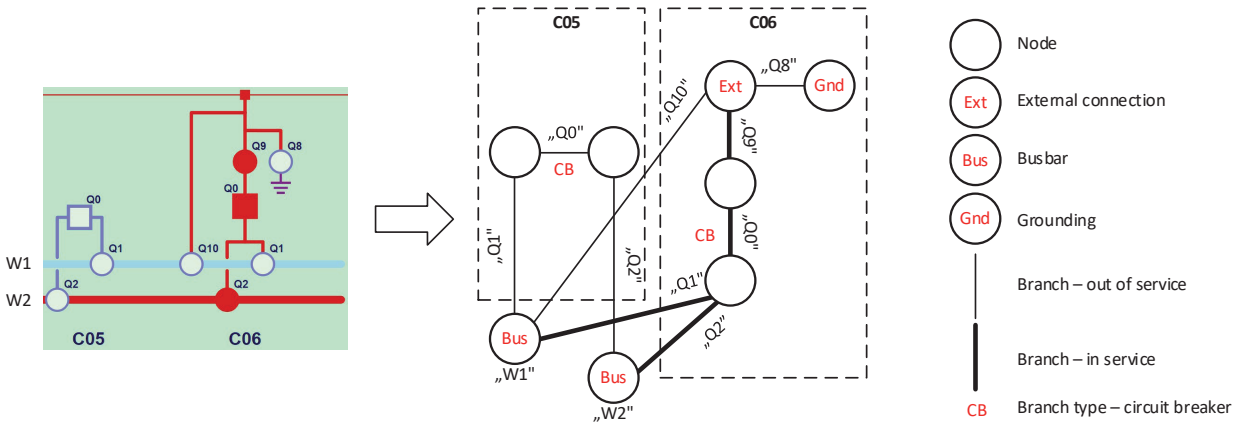


Fig. 2. Section of a single-line station scheme and the corresponding graph


Frano Tomašević, Vlatko Debeljuh, Renata Rubeša, Ana Jukić, Krešimir Mesić, Marko Kodrin, Bus Split Contingency Analysis Implementation in the NetVision DAM EMS, Journal of Energy, vol. 71 Number 3 (2022), 29–33
https://doi.org/10.37798/2022713422

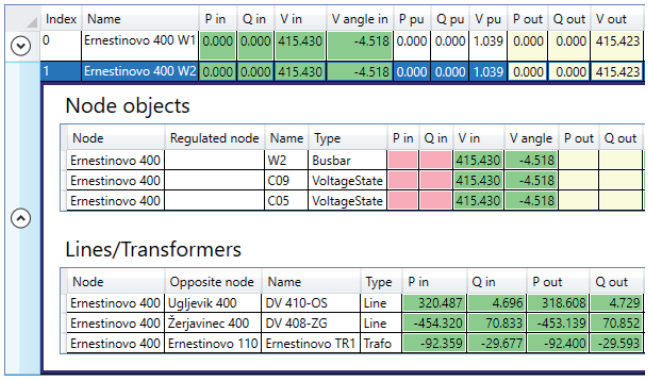


Fig. 3. Calculation subnodes for Ernestinovo 400 kV calculation node

NetVision DAM topology processor has been upgraded in order to detect the bus coupler paths within the substation graph. The modified DFS algorithm can be described in two steps:

1. Connection paths from each external connection point to busbars are detected. Branches leading from the external connection points to the busbars are marked as potential bus coupler paths.
2. Using the marked paths (step 1), connection paths from each busbar to another are detected. If a path includes a circuit breaker branch, it is declared a bus coupler.

First step is necessary in order to detect paths which represent disconnectors within bays which are not used as bus couplers.

After the DFS algorithm detects the connection components within the substation graph, additional analysis is used for defining the calculation subnodes which are connected by the bus coupler. Each calculation node with detected bus coupler has at least two calculation subnodes.

## IV. NetVision DAM contingency analysis

Contingency analysis calculation (N-1/N-2/N-k) is defined as a sequence of load flow calculations for predefined outages of a single or multiple elements which may endanger the operational security of a power system. Taking into account that the number of such outage scenarios can be very large, the speed of response can be considered as another important criterion, in addition to the accuracy, for the assessment of the quality of the contingency analysis calculations. Therefore, the conventional load flow algorithms, such as the Newton-Raphson or the Gauss-Seidel, should not be used for such task. In order to satisfy both conditions, modified versions of the conventional methods are used, in which the reduction of the execution time is achieved at the expense of minimal accuracy loss. Most often, the fast decoupled load flow (FDLF) is used [17].

FDLF is based on several effective simplifications of the standard Newton-Raphson algorithm, where the differences in the models are mostly manifested in the way the Jacobi (sub)matrices are calculated [18], [19]. In the FDLF algorithm, the Jacobi matrix is calculated only once, at the beginning of the iterative calculation. With the assumption of the weak coupling between the active power and the voltage magnitudes, on the one hand, and the reactive power and the voltage angle on the other, Jacobi submatrices J2 ($\partial P/\partial V$) and J3 ($\partial Q/\partial \delta$) are ignored. In this way the basic load flow system of equations can be separated into two independent systems. This assumption derives from several characteristics of the high-voltage transmission grid. Firstly, the phase angle differences between two adjacent nodes are very small ($\cos(\delta_i - \delta_j) \approx 1$). Secondly, the resistance and the reactance ratio (r/x), and the conductance and the susceptance ratio (g/b), are also relatively small ($r/x = g/b \ll 1$). Additional assumption is that the $G_{ij} \sin(\delta_i - \delta_j) \ll B_{ij}$ and the $Q_i \ll B_{ii} V_i^2$. While calculating the voltage angles the voltage magnitudes are usually set to the value of 1.0 p.u. Also, the ratios of the phase shifting transformers are ignored while calculating the voltage magnitudes. The basic mathematical model that follows from the above assumptions is given by the following equations:

$$B' \cdot \Delta\delta = \Delta P / V \tag{1}$$

$$B'' \cdot \Delta V = \Delta Q / V \tag{2}$$

It is important to point out that the Jacobi matrices B' and B'' are constant, and are calculated and factorized only once in the calculation (for the conventional outage scenarios).

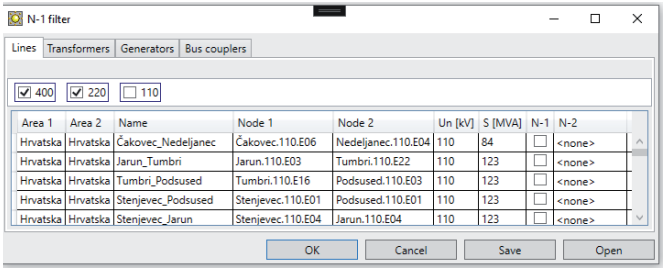


Fig. 4. Defining the N-1/N-2 outage scenarios in the NetVision DAM filter

NetVision DAM contingency analysis is calculated for the predefined N-1 and N-2 outage scenarios using the FDLF algorithm. The outage scenarios are defined using the appropriate contingency analysis filter, similarly for the on-line and the off-line calculations (Fig. 4). Currently, the user can select outages within the four groups of the power system elements: transmission lines and cables, transformers, generators and bus couplers. The filter list contains all the existing transmission grid objects and is created from the network model. Therefore, it does not depend on the analysed dynamic state. Selected objects which are not active in the analysed dynamic state are skipped within the contingency analysis. The same applies for the elements for which it is not possible to obtain the load flow results (i.e. outage of a critical branch separating the grid into two islands).

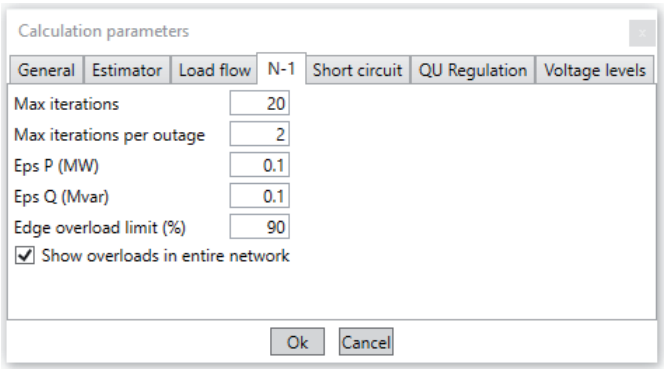


Fig. 5. Contingency analysis parameters in the NetVision DAM

Initial voltage values for each outage are taken from the base state (N-0), while the number of the iterations per outage is limited by the user settings. If the FDLF does not converge within the set


Frano Tomašević, Vlatko Debeljuh, Renata Rubeša, Ana Jukić, Krešimir Mesić, Marko Kodrin, Bus Split Contingency Analysis Implementation in the NetVision DAM
EMS, Journal of Energy, vol. 71 Number 3 (2022), 29–33
https://doi.org/10.37798/2022713422

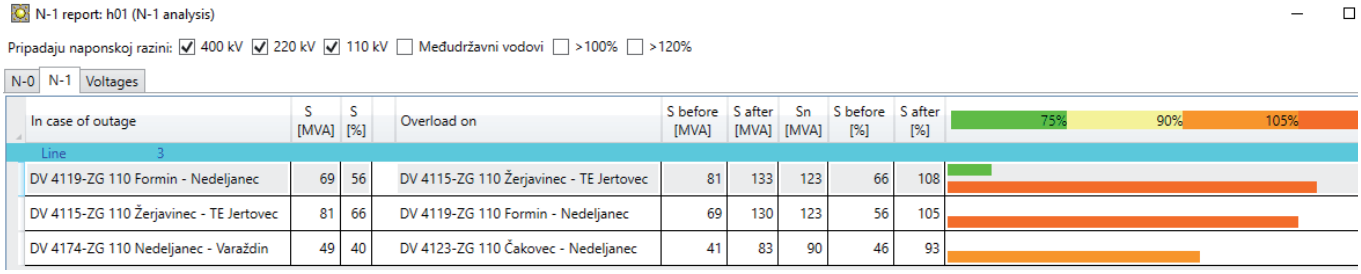


Fig. 6. List of the NetVision DAM N-0/N-1/N-2 alarms

number of iterations, however all the calculated electrical values are within the set boundaries, the calculation continues with the next outage. If some of the values are not within the set boundaries, the calculation continues till the convergence criteria is met. In this way, it is possible to quickly check and eliminate those outages that do not pose a danger to the system.

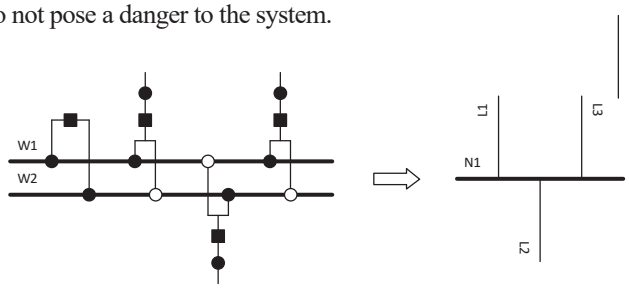


Fig. 7. Topological interpretation of the substation in case of active bus coupler

Calculation results for the outage scenarios in which some of the set constraints are violated are presented in the alarm interface (Fig. 6.). The results include the identification data of the outaged object, the object with the determined constraint violations, including the load flow results before and after the outage.

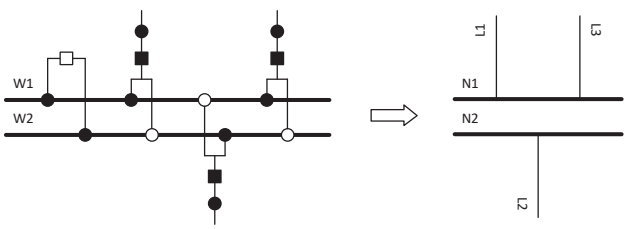


Fig. 8. Topological interpretation of the substation in case of inactive bus coupler

## V. Contingency analysis N-1 for bus coupler outages

Bus couplers connect busbar systems in the substation switchgear which have double or multiple busbars. The status of the bus coupler circuit breaker (active/inactive) defines the topological interpretation of the analysed substation state. In case of the active bus coupler (Fig. 7.), the incident busbars W1 and W2 are at the same electric potential, so the result of the topological analysis is only one computational node – N1, incident with three calculation branches L1 – L3.

In case of inactive bus coupler (Fig. 8.), the final result of the topological analysis are two separated calculation nodes – N1 and N2, where N1 is incident with branches L1 and L3, and N2 with branch L2.

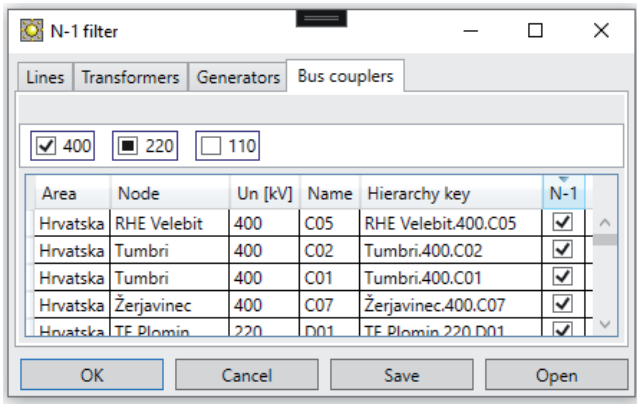


Fig. 9. Defining the NetVision DAM N-1 bus coupler outages

N-1 contingency analysis calculations for the bus coupler outages require a change in the number of the calculation nodes. Therefore, mathematical models are significantly more complex in comparison with other outage scenarios. In addition, standard calculation model does not contain the bus coupler as an independent calculation object, as it is usually an invisible part of the calculation node (Fig. 7.).

Modifications of the NetVision DAM topological processor and the calculation model enabled the identification of the bus couplers and the creation of calculation subnodes. Calculation subnode and the bus coupler data are stored within the extended data of the associated calculation node. In case of a bus coupler outage, the subnodes are transformed from the potential to the real calculation nodes, while the original calculation node is removed from the calculation model. In this way, all the prerequisites for the contingency calculation are provided directly in the calculation model. Bus coupler outages are selected within the filter list, in the same way as all the other N-1 objects (Fig. 9.).

A change in the calculation node list requires a significant modification of the whole calculation model. Considering the implementation issues solely, much simpler approach would be to directly change the dynamic state, i.e. the topology state of the network model, and then create the new calculation model [20], [21]. However, such approach would be burdensome, and would require much longer time of execution. Therefore, it is more acceptable to make such changes directly on the calculation model, by resizing and recalculating (input and output) vectors and matrices Y, B' and B''. Modifications of the vectors and matrices are additionally conditioned by the types of the new nodes (PV, PQ, REF). Modifications of the FDLF model are illustrated by equations (3) and (4).

In case of the bus coupler outage in the node *k* (red), two new nodes (green) are created from the predefined subnodes, and the initial parent node is removed from the model. Initial Jacobi matrices B' and B'' need to be modified and refactored, which is the most demanding and the most time-consuming part of the calculation.


Frano Tomašević, Vlatko Debeljuh, Renata Rubeša, Ana Jukić, Krešimir Mesić, Marko Kodrin, Bus Split Contingency Analysis Implementation in the NetVision DAM EMS, Journal of Energy, vol. 71 Number 3 (2022), 29–33
https://doi.org/10.37798/2022713422

$$B'_{[(n-1)\times(n-1)]} \cdot \begin{vmatrix} \Delta\delta_1 \\ \vdots \\ \Delta\delta_k^{(node)} \\ \vdots \\ \Delta\delta_{n-1} \end{vmatrix} = \begin{vmatrix} \frac{\Delta P_1}{V_1} \\ \vdots \\ \frac{\Delta P_k^{(node)}}{V_k^{(node)}} \\ \vdots \\ \frac{\Delta P_{n-1}}{V_{n-1}} \end{vmatrix} \Rightarrow B'_{[n\times n]} \cdot \begin{vmatrix} \Delta\delta_1 \\ \vdots \\ \Delta\delta_k^{(subn\ 1)} \\ \Delta\delta_{k+1}^{(subn\ 2)} \\ \vdots \\ \Delta\delta_n \end{vmatrix} = \begin{vmatrix} \frac{\Delta P_1}{V_1} \\ \vdots \\ \frac{\Delta P_k^{(subn\ 1)}}{\Delta V_k^{(subn\ 1)}} \\ \frac{\Delta P_{k+1}^{(subn\ 2)}}{\Delta V_{k+1}^{(subn\ 2)}} \\ \vdots \\ \frac{\Delta P_n}{V_n} \end{vmatrix} \quad (3)$$

$$B''_{[(n-g-1)\times(n-g-1)]} \cdot \begin{vmatrix} \Delta V_1 \\ \vdots \\ \Delta V_k^{(node)} \\ \vdots \\ \Delta V_{n-g-1} \end{vmatrix} = \begin{vmatrix} \frac{\Delta Q_1}{V_1} \\ \vdots \\ \frac{\Delta Q_k^{(node)}}{V_k^{(node)}} \\ \vdots \\ \frac{\Delta Q_{n-g-1}}{V_{n-g-1}} \end{vmatrix} \Rightarrow B''_{[(n-g)\times(n-g)]} \cdot \begin{vmatrix} \Delta V_1 \\ \vdots \\ \Delta V_k^{(subn\ 1)} \\ \Delta V_{k+1}^{(subn\ 2)} \\ \vdots \\ \Delta V_{n-g} \end{vmatrix} = \begin{vmatrix} \frac{\Delta Q_1}{V_1} \\ \vdots \\ \frac{\Delta Q_k^{(subn\ 1)}}{\Delta V_k^{(subn\ 1)}} \\ \frac{\Delta Q_{k+1}^{(subn\ 2)}}{\Delta V_{k+1}^{(subn\ 2)}} \\ \vdots \\ \frac{\Delta Q_{n-g}}{V_{n-g}} \end{vmatrix} \quad (4)$$

## VI. Conclusion

Implementation of the bus coupler outage scenarios in the N-1 contingency analysis requires specific modifications of the calculation model. In order to identify the bus couplers in the network model, the topology processor was upgraded. If the bus couplers have been identified, new calculation objects – subnodes, are created based on the topology analysis results. Subnodes are potential nodes, which transform into real ones when the incident bus coupler is not active. The basic subnode data (i.e. branch and node object incidents) is stored within the calculation node data. In this way, just by modifying the existing calculation model, all the basic prerequisites for the implementation of the bus coupler outages in the contingency analysis N-1 are met. The mathematical analysis of the bus coupler outage scenario requires the modifications of the input matrices and vectors, whereby their dimensions increase due to the increase of the number of the calculation nodes. The need for the refactorization of the Jacobi matrices is the main drawback of this mathematical approach. However, this solution is superior to the alternative in which the calculation model is not modified, but instead created from the scratch, with the status of the analysed bus coupler set to inactive. This approach would require much longer execution time, and as such would therefore be inapplicable.

## References


[1] V. Kekatos and G. B. Giannakis, "Joint power system state estimation and breaker status identification," in *Proc. North American Power Symp.*, 2012.

[2] G. Korres, P. Katsikas, and G. Chatzarakis, "Substation topology identification in generalized state estimation," International Journal of Electrical Power & Energy Systems, vol. 28, no. 3, pp. 195–206, 2006.

[3] D. Deka, R. Baldick, and S. Vishwanath, "One breaker is enough: Hidden topology attacks on power grids," in *Proc. IEEE PES General Meeting*, 2015.

[4] C.-W. Ten, K. Yamashita, Z. Yang, A. V. Vasilakos, and A. Ginter, "Impact assessment of hypothesized cyberattacks on interconnected bulk power systems," IEEE Trans. Smart Grid, vol. 9, no. 5, 2017.

[5] Y. Zhou, J. Cisneros-Saldana, and L. Xie, "False analog data injection attack towards topology errors: Formulation and feasibility analysis," in *Proc. IEEE PES General Meeting*, 2018.

[6] A. A. Jahromi, A. Kemmeugne, D. Kundur, and A. Haddadi, "Cyber-physical attacks targeting communication-assisted protection schemes," IEEE Trans. Power Systems, vol. 35, no. 1, pp. 440–450, 2019.

[7] Y. Zhou, A. S. Zamzam, A. Bernstein, and H. Zhu, "Substation-Level Grid Topology Optimization Using Bus Splitting", in *2021 American Control Conference (ACC)*, New Orleans, USA, May 25-28, 2021.

[8] A. J. Wood, B. F. Wollenberg, and G. B. Sheble, *Power generation, operation, and control*. John Wiley & Sons, 2013.

[9] A. A. Mazi, B. F. Wollenberg, and M. H. Hesse, "Corrective control of power system flows by line and bus-bar switching", IEEE Trans Power Syst., vol. 1, no. 3, pp. 258-264, 1986.

[10] K. N. Wrubel, P. S. Rapcienski, K. L. Lee, B. S. Gisin, and G. W. Woodzell, "Practical experience with corrective switching algorithm for on-line applications", IEEE Trans Power Syst, vol. 11, no. 1, pp. 415-421, 1996.

[11] W. Shao, V. Vittal, "Corrective switching algorithm for relieving overloads and voltage violations", IEEE Trans Power Syst., vol. 20, no. 4, pp. 1877-1885, 2005.

[12] Y. Zhou, H. Zhu, "Bus Split Sensitivity Analysis for Enhanced Security in Power System Operations", in *2019 North American Power Symposium (NAPS)*, Wichita, KS, USA, October 13-15, 2019.

[13] Y. Pradeep, P. Seshuraju, S. A. Khaparde, and R. K. Joshi, "Cim-based connectivity model for bus-branch topology extraction and exchange," IEEE Trans. Smart Grid, vol. 2, no. 2, pp. 244-253, 2011.

[14] B. Park, J. Holzer, and C. L. DeMarco, "A sparse tableau formulation for node-breaker representations in security-constrained optimal power flow," IEEE Trans. Power Systems, vol. 34, no. 1, pp. 637--647, 2019.

[15] S. Even, G. Even, *Graph Algorithms*, New York: Cambridge University Press, 1979

[16] A. Bony, U. S. R. Murty, *Graph Theory*, London, Springer-Verlag London, 2008

[17] B. Stott, C. Alsac, "Fast Decoupled Load Flow", *IEEE Transactions on Power Apparatus and Systems*, vol. PAS-93, no. 3, May 1974., pp 859-869

[18] A. Gomez Exposito, A. J. Conejo, C. Canizares, *Electric Energy Systems Analysis and Operation*, Boca Raton, FL: Taylor & Francis Group, LLC, USA, 2009

[19] J. J. Grainger, W. D. Stevenson, *Power System Analysis*, ., New York: McGraw-Hill, Inc, 1994

[20] R. Ramanathan, B. Tuck, "Contingency analysis using node/breaker model for operation studies", in *2015 IEEE Power & Energy Society General Meeting*, Denver, CO, USA, July, 2015.

[21] R. Ramanathan, B. Tuck," BPA's Experience of Implementing Node Breaker Model for Power System Operations Studies", *International Universities Power Engineering Conference (UPEC) 2013,* Dublin, Ireland, Sept., 2013

# ENERGIJA